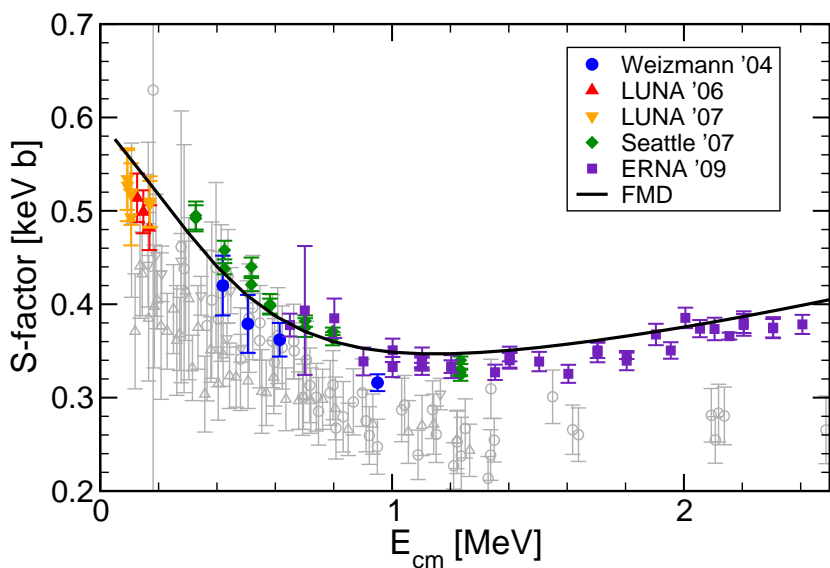


Clusters and Halos in Structure and Reactions of light Nuclei studied in FMD



Thomas Neff
**“Localization and Clustering
in Atomic Nuclei”**
ESNT Workshop
CEA/SPhN Saclay, France
May 29-30, 2013

Overview



Unitary Correlation Operator Method

Fermionic Molecular Dynamics

Localization and Clustering

$^3\text{He}(\alpha, \gamma)^7\text{Be}$ Radiative Capture Reaction

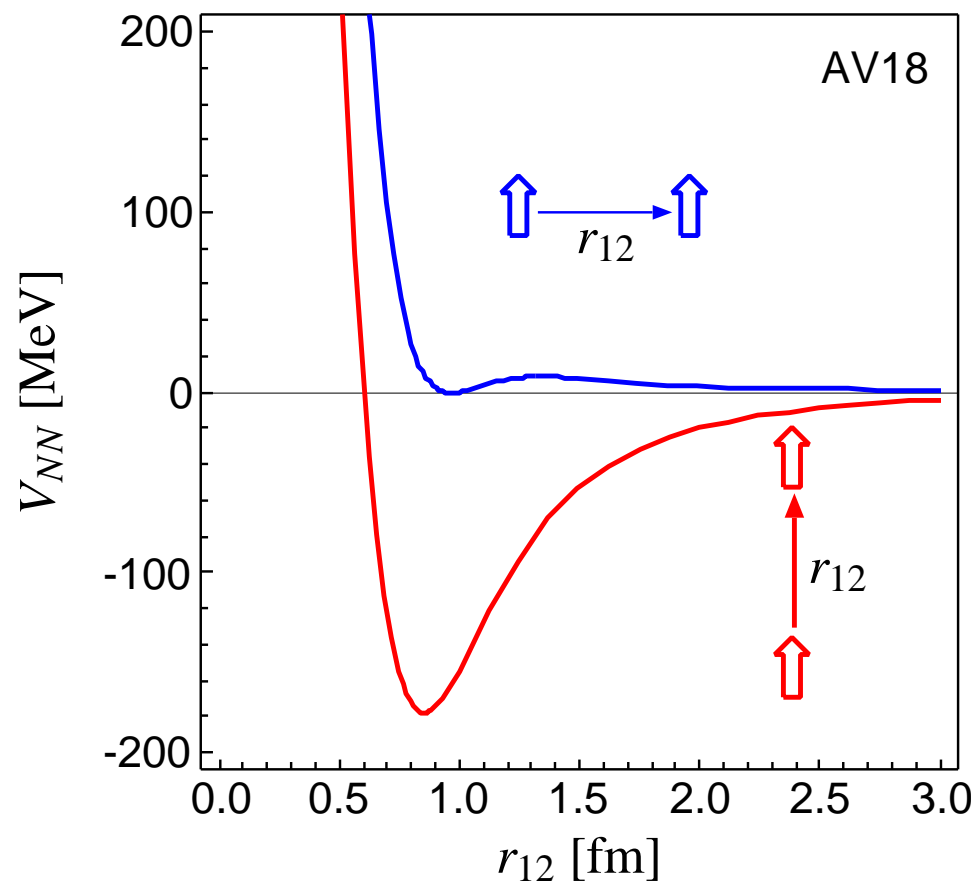
Cluster States in ^{12}C

Neon Isotopes – Halo-candidate ^{17}Ne

Nuclear Force

Argonne V18 ($T=0$)

spins aligned parallel or perpendicular to the relative distance vector



- strong repulsive core:
nucleons can not get closer
than ≈ 0.5 fm

➡ **central correlations**

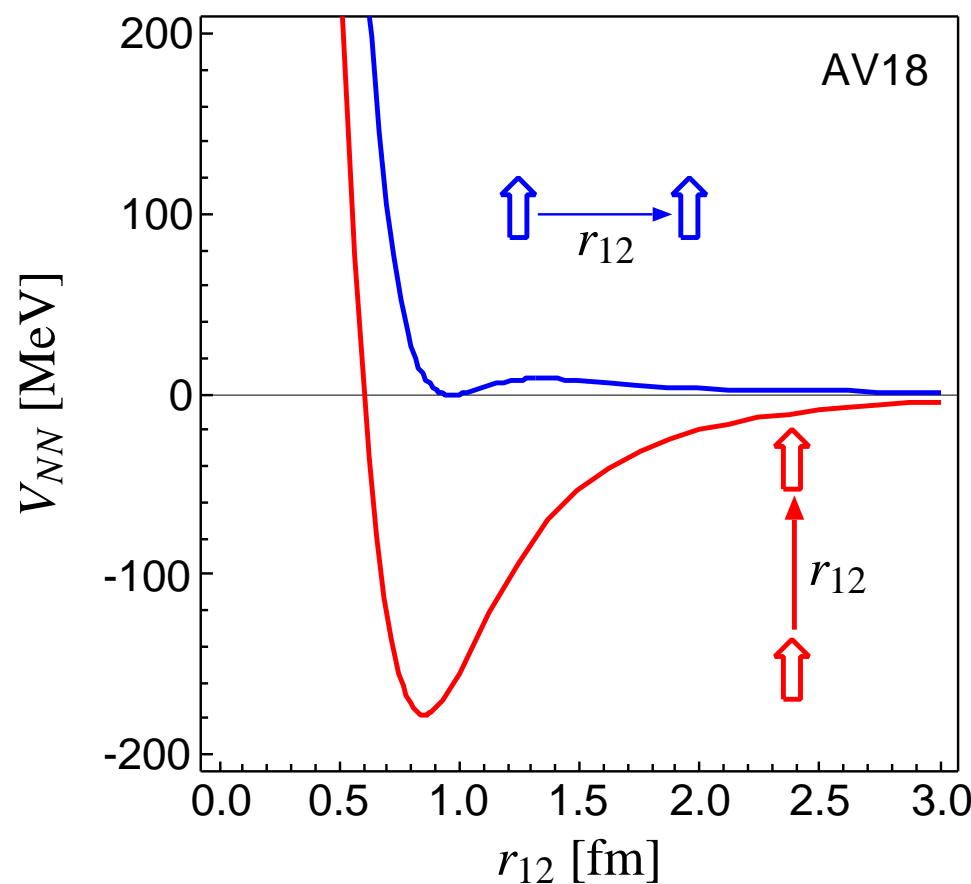
- strong dependence on the orientation of the spins due
to the tensor force

➡ **tensor correlations**

Nuclear Force

Argonne V18 ($T=0$)

spins aligned parallel or perpendicular to the relative distance vector



- strong repulsive core:
nucleons can not get closer
than ≈ 0.5 fm

➡ **central correlations**

- strong dependence on the orientation of the spins due
to the tensor force

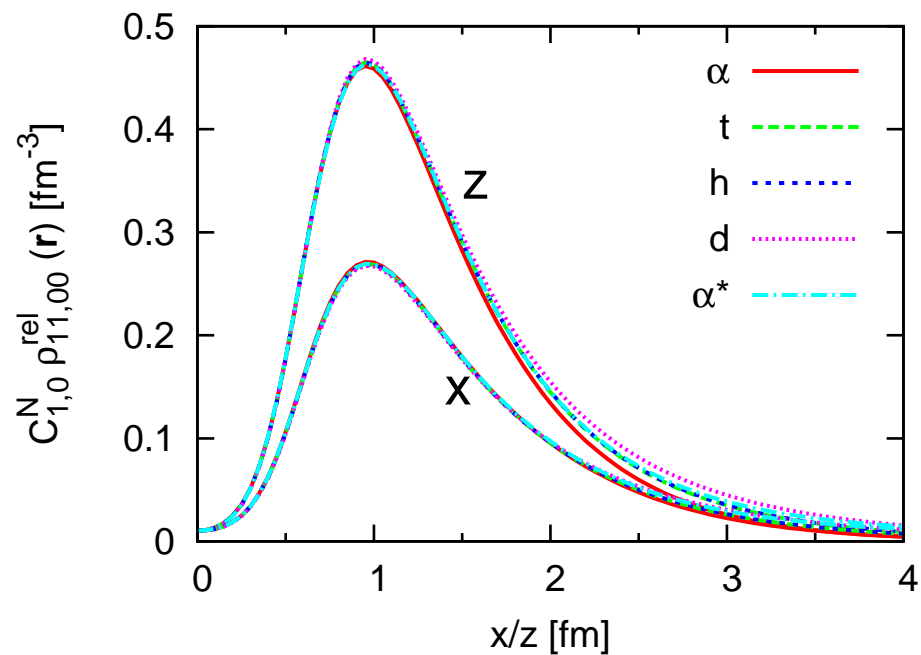
➡ **tensor correlations**

the nuclear force will induce
strong short-range correlations in the nuclear
wave function

- Universality of short-range correlations
- Two-body densities in $A = 2, 3, 4$ Nuclei — AV8'

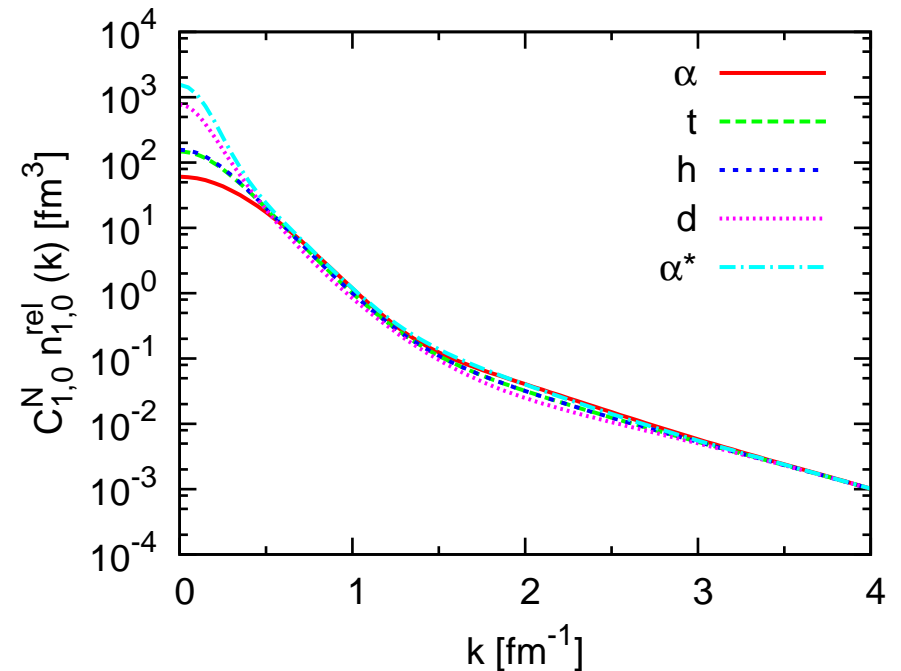
coordinate space

$$S = 1, M_S = 1, T = 0$$



momentum space

$$S = 1, T = 0$$



- normalize two-body density in coordinate space at $r=1.0$ fm
- normalized two-body densities in coordinate space are identical at short distances for all nuclei
- use the **same** normalization factor in momentum space – high momentum tails agree for all nuclei

Unitary Correlation Operator Method

Correlation Operator

- induce short-range (two-body) central and tensor correlations into the many-body state

$$\tilde{C} = \tilde{\zeta}_\Omega \tilde{\zeta}_r = \exp[-i \sum_{i < j} \tilde{g}_{\Omega,ij}] \exp[-i \sum_{i < j} \tilde{g}_{r,ij}] \quad , \quad \tilde{C}^\dagger \tilde{C} = \mathbb{1}$$

- correlation operator should conserve the symmetries of the Hamiltonian and should be of finite-range, correlated interaction **phase shift equivalent** to bare interaction by construction

Correlated Operators

- correlated operators will have contributions in higher cluster orders

$$\tilde{C}^\dagger \tilde{Q} \tilde{C} = \hat{Q}^{[1]} + \hat{Q}^{[2]} + \hat{Q}^{[3]} + \dots$$

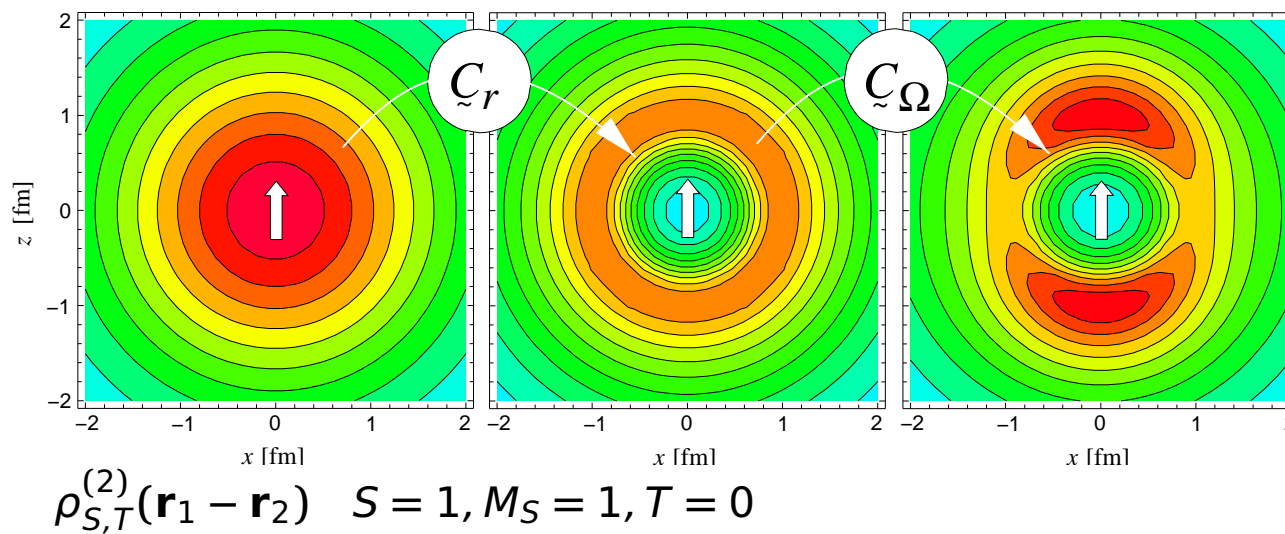
- two-body approximation: correlation range should be small compared to mean particle distance

Correlated Interaction

$$\tilde{C}^\dagger (\tilde{T} + \tilde{V}) \tilde{C} = \tilde{T} + \tilde{V}_{\text{UCOM}} + \tilde{V}_{\text{UCOM}}^{[3]} + \dots$$

- Unitary Correlation Operator Method
- Correlations and Energies

two-body densities

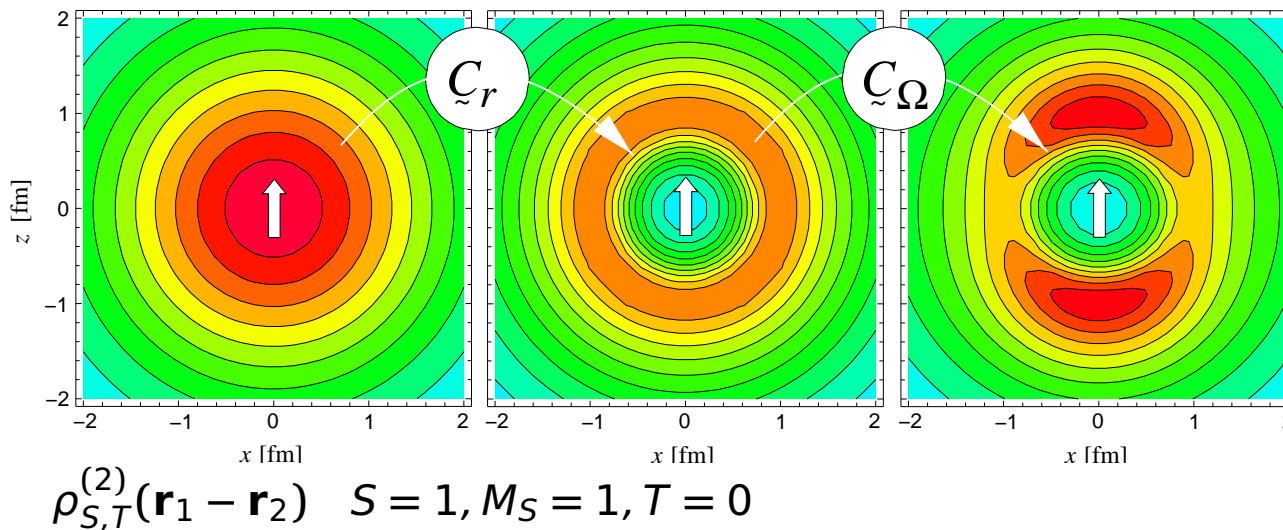


central correlator \tilde{C}_r
shifts density out of
the repulsive core

tensor correlator \tilde{C}_Ω
aligns density with spin
orientation

- Unitary Correlation Operator Method
- Correlations and Energies

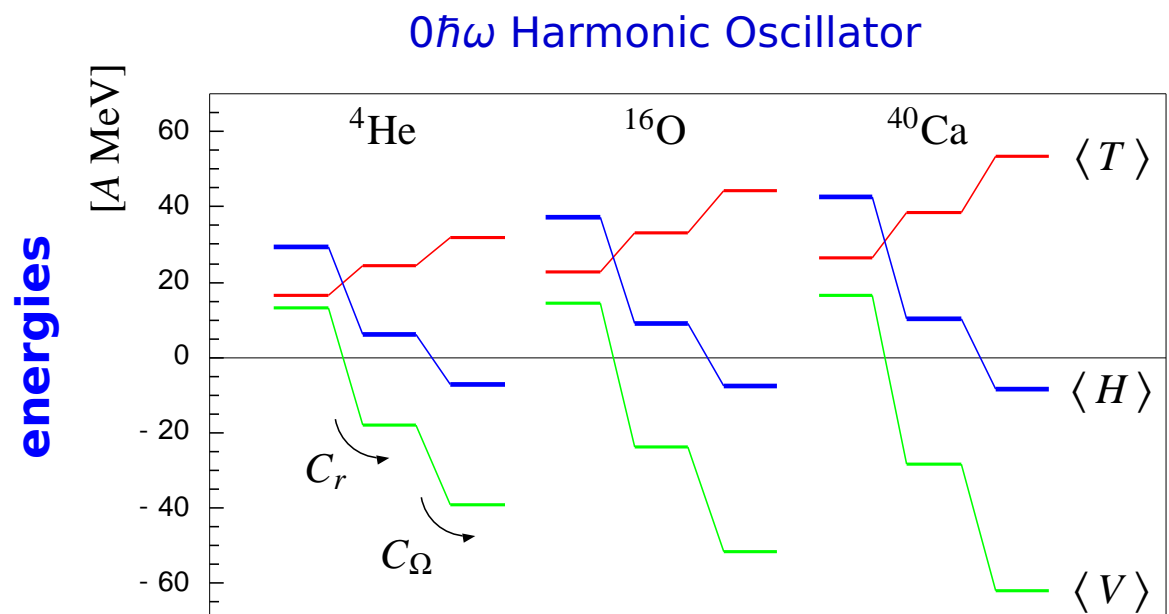
two-body densities



central correlator \tilde{C}_r
shifts density out of
the repulsive core

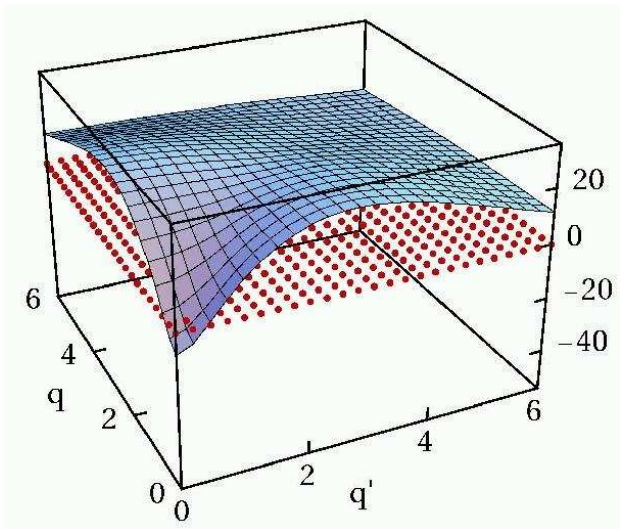
tensor correlator \tilde{C}_Ω
aligns density with spin
orientation

both central
and tensor
correlations are
essential for
binding



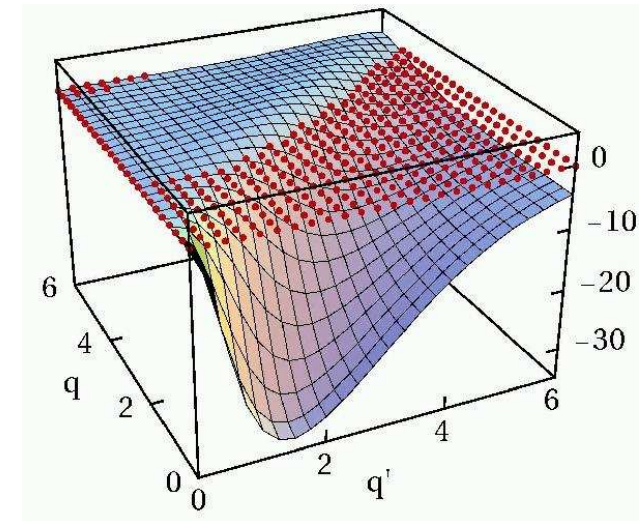
- Unitary Correlation Operator Method
- Correlated Interaction in Momentum Space

3S_1 bare



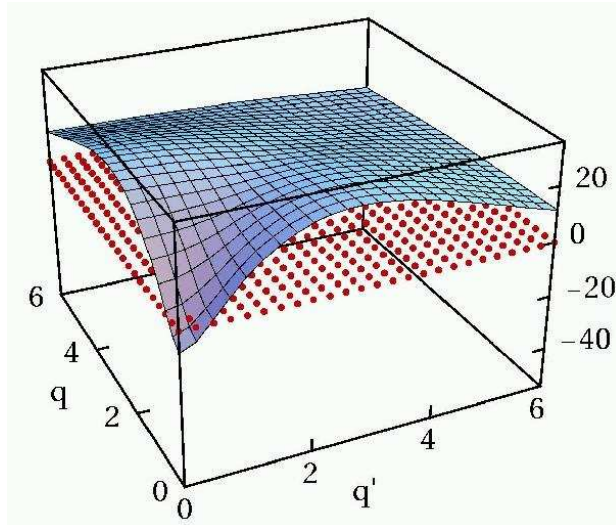
bare interaction has
strong
off-diagonal matrix
elements connecting
to high momenta

$^3S_1 - ^3D_1$ bare



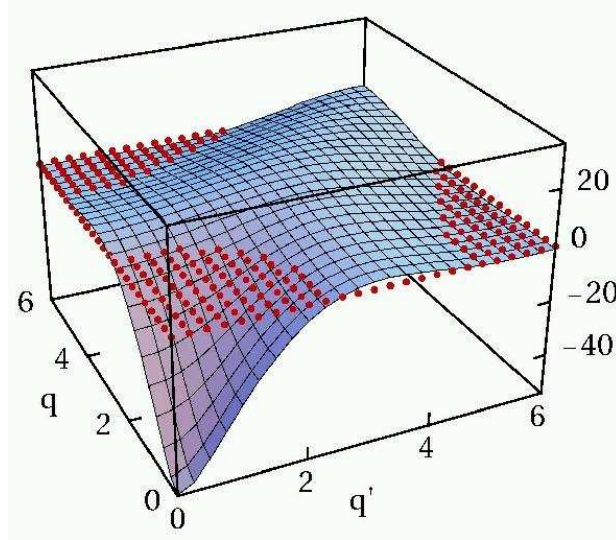
- Unitary Correlation Operator Method
- Correlated Interaction in Momentum Space

3S_1 bare



bare interaction has
strong off-diagonal matrix
elements connecting
to high momenta

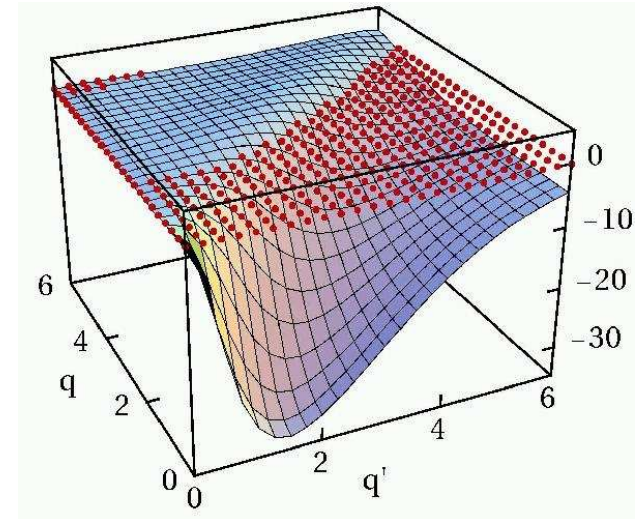
3S_1 correlated



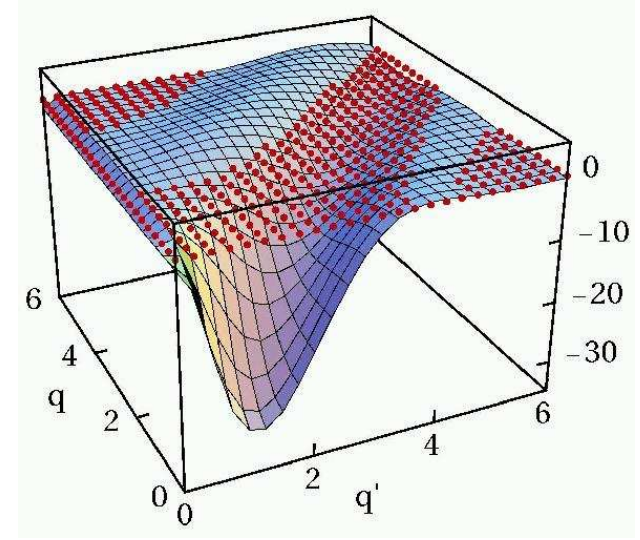
correlated interaction
is **more attractive**
at low momenta

**off-diagonal
matrix elements**
connecting low- and
high- momentum
states are **strongly
reduced**

$^3S_1 - ^3D_1$ bare

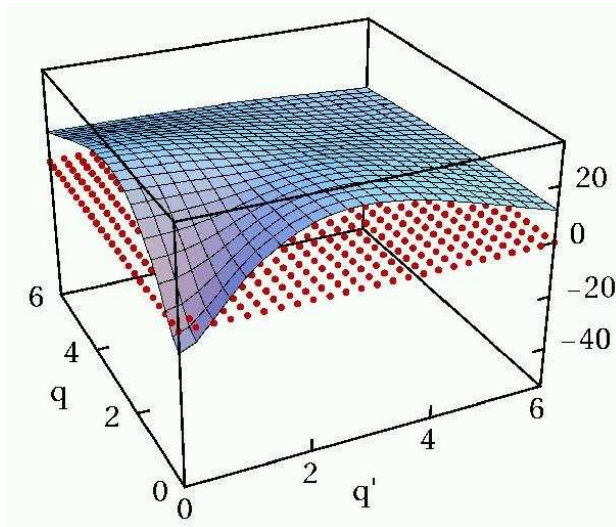


$^3S_1 - ^3D_1$ correlated



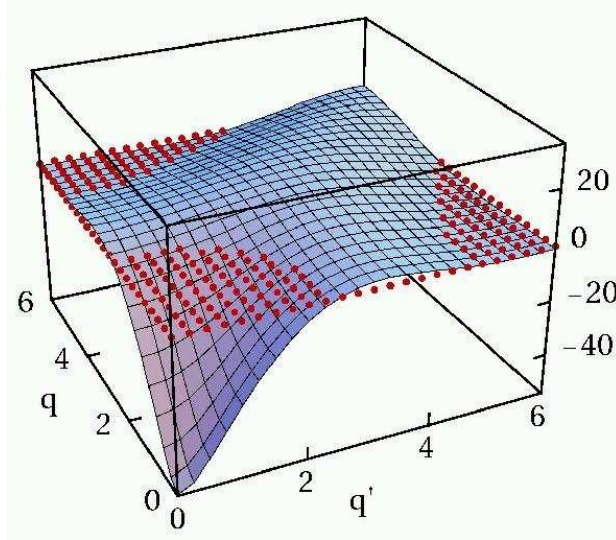
- Unitary Correlation Operator Method
- Correlated Interaction in Momentum Space

3S_1 bare



bare interaction has
strong off-diagonal matrix elements connecting to high momenta

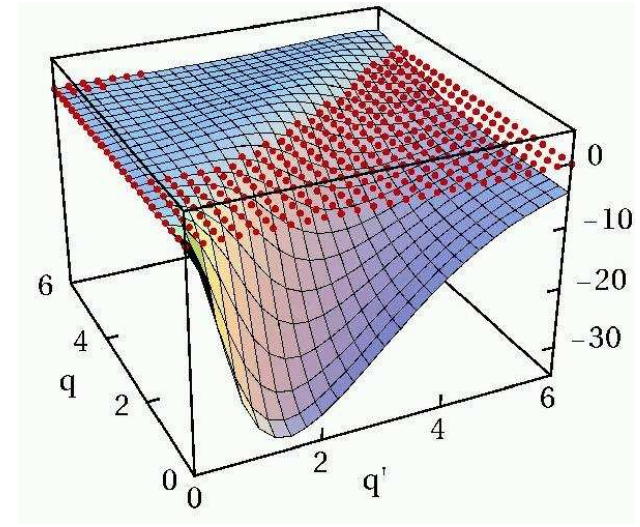
3S_1 correlated



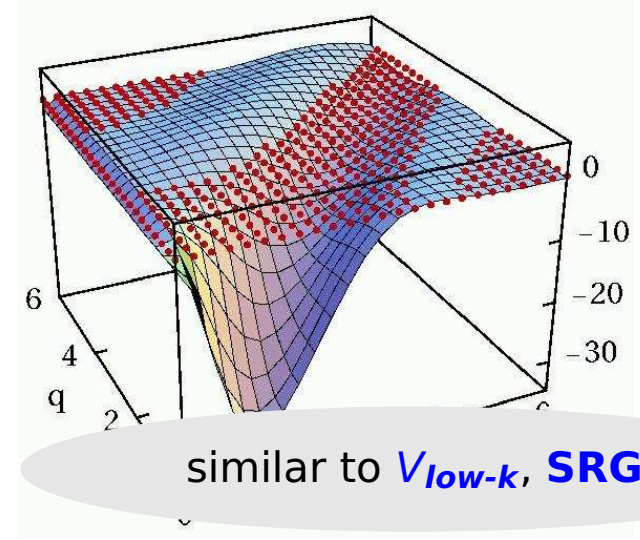
correlated interaction is **more attractive** at low momenta

off-diagonal matrix elements connecting low- and high-momentum states are **strongly reduced**

$^3S_1 - ^3D_1$ bare

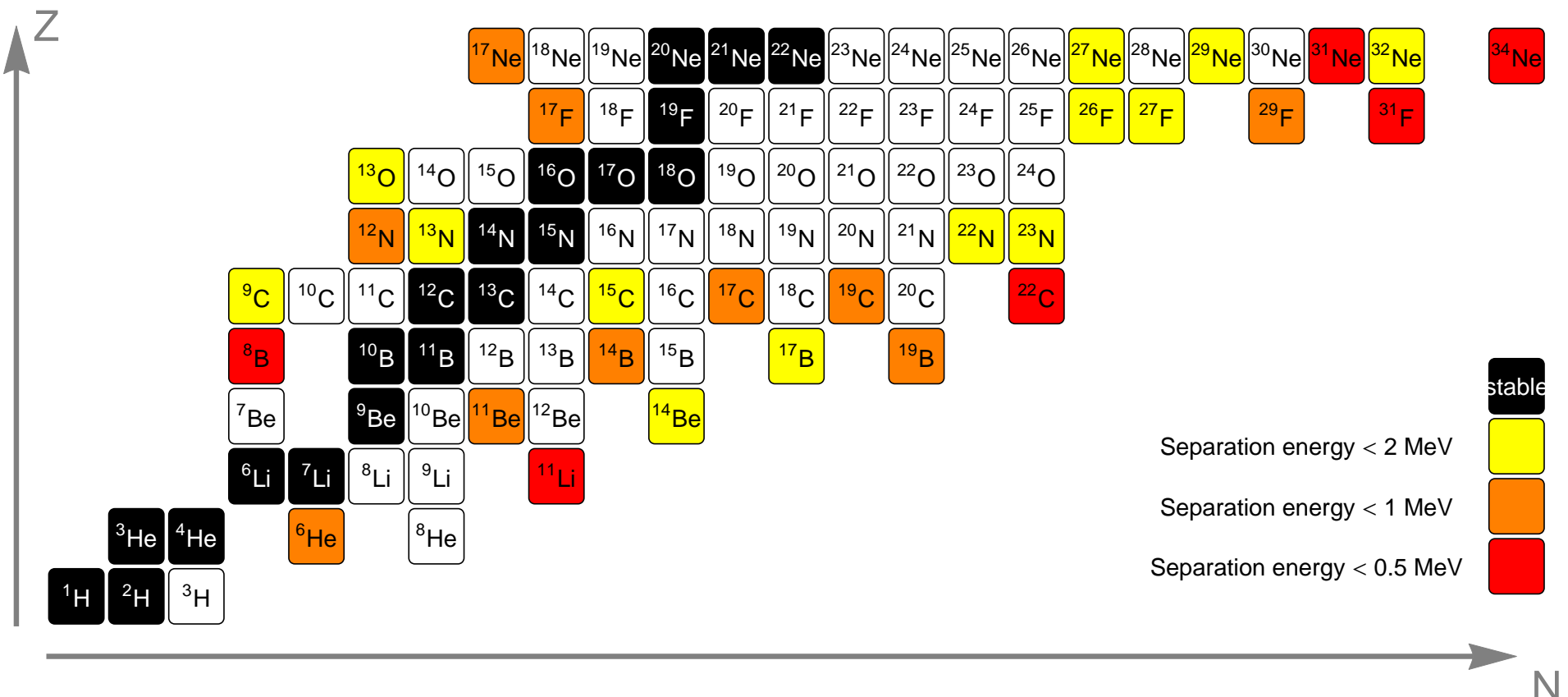


$^3S_1 - ^3D_1$ correlated



similar to V_{low-k} , SRG

Exotica: Special Challenges



- states close to one-nucleon, two-nucleon or cluster thresholds can have well developed **halo** or **cluster** structure
- these are hard to tackle in the harmonic oscillator basis

• FMD

• Fermionic Molecular Dynamics

Fermionic

Slater determinant

$$|Q\rangle = \mathcal{A}(|q_1\rangle \otimes \cdots \otimes |q_A\rangle)$$

- antisymmetrized A -body state

Feldmeier, Schnack, Rev. Mod. Phys. **72** (2000) 655

Neff, Feldmeier, Nucl. Phys. **A738** (2004) 357

Fermionic Molecular Dynamics

Fermionic

Slater determinant

$$|Q\rangle = \mathcal{A} \left(|q_1\rangle \otimes \cdots \otimes |q_A\rangle \right)$$

- antisymmetrized A -body state

Molecular

single-particle states

$$\langle \mathbf{x} | q \rangle = \sum_i c_i \exp \left\{ -\frac{(\mathbf{x} - \mathbf{b}_i)^2}{2a_i} \right\} \otimes |x_{i+}^{\uparrow}, x_{i-}^{\downarrow}\rangle \otimes |\xi\rangle$$

- Gaussian wave-packets in phase-space (complex parameter \mathbf{b}_i encodes mean position and mean momentum), spin is free, isospin is fixed
- width a_i is an independent variational parameter for each wave packet
- use one or two wave packets for each single particle state

Feldmeier, Schnack, Rev. Mod. Phys. **72** (2000) 655

Neff, Feldmeier, Nucl. Phys. **A738** (2004) 357

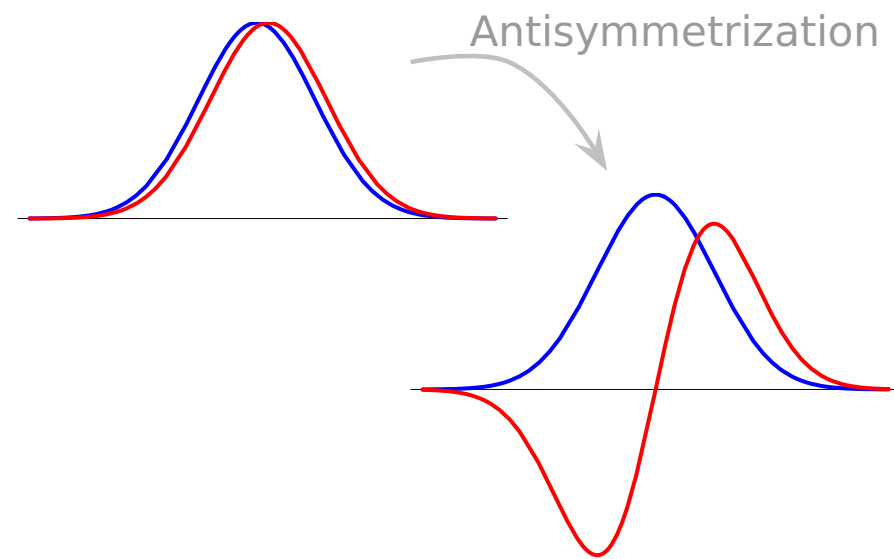
Fermionic Molecular Dynamics

Fermionic

Slater determinant

$$|Q\rangle = \mathcal{A} \left(|q_1\rangle \otimes \cdots \otimes |q_A\rangle \right)$$

- antisymmetrized A -body state



Molecular

single-particle states

$$\langle \mathbf{x} | q \rangle = \sum_i c_i \exp\left\{-\frac{(\mathbf{x} - \mathbf{b}_i)^2}{2a_i}\right\} \otimes |x_{i+}^{\uparrow}, x_{i-}^{\downarrow}\rangle \otimes |\xi\rangle$$

- Gaussian wave-packets in phase-space (complex parameter \mathbf{b}_i encodes mean position and mean momentum), spin is free, isospin is fixed
- width a_i is an independent variational parameter for each wave packet
- use one or two wave packets for each single particle state

Feldmeier, Schnack, Rev. Mod. Phys. **72** (2000) 655

Neff, Feldmeier, Nucl. Phys. **A738** (2004) 357

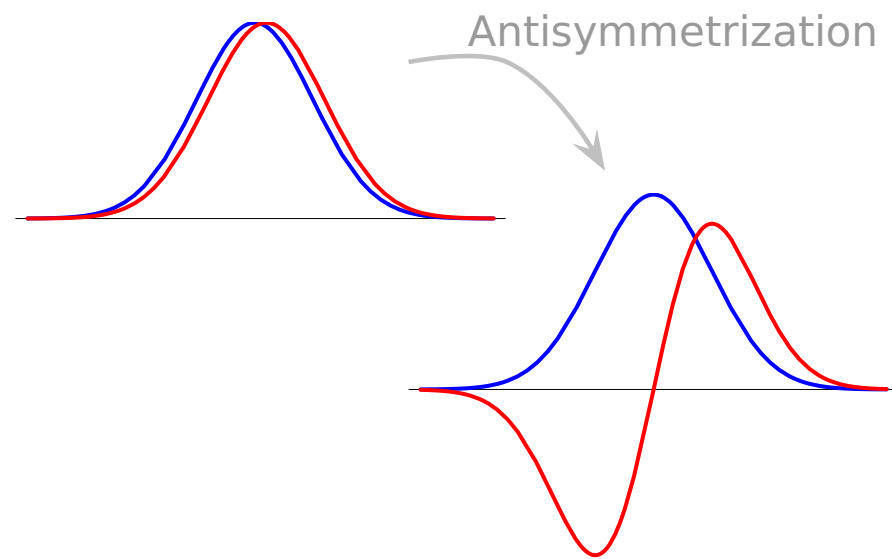
Fermionic Molecular Dynamics

Fermionic

Slater determinant

$$|Q\rangle = \mathcal{A} \left(|q_1\rangle \otimes \cdots \otimes |q_A\rangle \right)$$

- antisymmetrized A -body state



Molecular

single-particle states

$$\langle x | q \rangle = \sum_i c_i \exp\left\{-\frac{(x - b_i)^2}{2a_i}\right\} \otimes |x_{i+}^{\uparrow}, x_{i-}^{\downarrow}\rangle \otimes |\xi\rangle$$

- Gaussian wave-packets in phase-space (complex parameter b_i encodes mean position and mean momentum), spin is free, isospin is fixed
- width a_i is an independent variational parameter for each wave packet
- use one or two wave packets for each single particle state

see also
**Antisymmetrized
Molecular Dynamics**
Horiuchi, Kanada-En'yo,
Kimura, ...

Feldmeier, Schnack, Rev. Mod. Phys. **72** (2000) 655

Neff, Feldmeier, Nucl. Phys. **A738** (2004) 357

Interaction Matrix Elements

(One-body) Kinetic Energy

$$\langle q_k | \mathcal{T} | q_l \rangle = \langle a_k b_k | \mathcal{T} | a_l b_l \rangle \langle x_k | x_l \rangle \langle \xi_k | \xi_l \rangle$$

$$\langle a_k b_k | \mathcal{T} | a_l b_l \rangle = \frac{1}{2m} \left(\frac{3}{a_k^* + a_l} - \frac{(b_k^* - b_l)^2}{(a_k^* + a_l)^2} \right) R_{kl}$$

(Two-body) Potential

► fit radial dependencies by (a sum of) Gaussians

$$G(\mathbf{x}_1 - \mathbf{x}_2) = \exp\left\{-\frac{(\mathbf{x}_1 - \mathbf{x}_2)^2}{2\kappa}\right\}$$

► Gaussian integrals

$$\langle a_k b_k, a_l b_l | G | a_m b_m, a_n b_n \rangle = R_{km} R_{ln} \left(\frac{\kappa}{\alpha_{klmn} + \kappa} \right)^{3/2} \exp\left\{-\frac{\rho_{klmn}^2}{2(\alpha_{klmn} + \kappa)}\right\}$$

► analytical expressions for matrix elements

$$\alpha_{klmn} = \frac{a_k^* a_m}{a_k^* + a_m} + \frac{a_l^* a_n}{a_l^* + a_n}$$

$$\rho_{klmn} = \frac{a_m b_k^* + a_k^* b_m}{a_k^* + a_m} - \frac{a_n b_l^* + a_l^* b_n}{a_l^* + a_n}$$

$$R_{km} = \langle a_k b_k | a_m b_m \rangle$$

Operator Representation of V_{UCOM}

$$\tilde{C}^\dagger (\mathcal{T} + \tilde{V}) \tilde{C} = \mathcal{T}$$

$$+ \sum_{ST} \hat{V}_c^{ST}(r) + \frac{1}{2} (\tilde{p}_r^2 \hat{V}_{p^2}^{ST}(r) + \hat{V}_{p^2}^{ST}(r) \tilde{p}_r^2) + \hat{V}_{l^2}^{ST}(r) \mathbf{l}^2$$

one-body kinetic energy

$$+ \sum_T \hat{V}_{ls}^T(r) \mathbf{l} \cdot \mathbf{s} + \hat{V}_{l^2 ls}^T(r) \mathbf{l}^2 \mathbf{l} \cdot \mathbf{s}$$

central potentials

$$+ \sum_T \hat{V}_t^T(r) \tilde{S}_{12}(\mathbf{r}, \mathbf{r}) + \hat{V}_{trp_\Omega}^T(r) \tilde{p}_r \tilde{S}_{12}(\mathbf{r}, \mathbf{p}_\Omega) + \hat{V}_{tll}^T(r) \tilde{S}_{12}(\mathbf{l}, \mathbf{l}) + \\ \hat{V}_{tp_\Omega p_\Omega}^T(r) \tilde{S}_{12}(\mathbf{p}_\Omega, \mathbf{p}_\Omega) + \hat{V}_{l^2 tp_\Omega p_\Omega}^T(r) \mathbf{l}^2 \tilde{S}_{12}(\mathbf{p}_\Omega, \mathbf{p}_\Omega)$$

spin-orbit potentials

tensor potentials

bulk of tensor force mapped onto central part
of correlated interaction

tensor correlations also change the spin-orbit
part of the interaction

• FMD

• PAV, VAP and Multiconfiguration

Projection After Variation (PAV)

- mean-field may break symmetries of Hamiltonian
- restore inversion, translational and rotational symmetry by projection on parity, linear and angular momentum

$$\tilde{P}^\pi = \frac{1}{2}(1 + \pi \tilde{\Pi})$$

$$\tilde{P}_{MK}^J = \frac{2J+1}{8\pi^2} \int d^3\Omega D_{MK}^J(\Omega) \tilde{R}(\Omega)$$

$$\tilde{P}^{\mathbf{P}} = \frac{1}{(2\pi)^3} \int d^3X \exp\{-i(\tilde{\mathbf{P}} - \mathbf{P}) \cdot \mathbf{X}\}$$

• PAV, VAP and Multiconfiguration

Projection After Variation (PAV)

- mean-field may break symmetries of Hamiltonian
- restore inversion, translational and rotational symmetry by projection on parity, linear and angular momentum

$$\tilde{P}^\pi = \frac{1}{2}(1 + \pi\tilde{\Pi})$$

$$\tilde{P}_{MK}^J = \frac{2J+1}{8\pi^2} \int d^3\Omega D_{MK}^J(\Omega) \tilde{R}(\Omega)$$

Variation After Projection (VAP)

- effect of projection can be large
- **Variation after Angular Momentum and Parity Projection** (VAP) for light nuclei
- combine VAP with **constraints** on **radius**, **dipole** moment, **quadrupole** moment, ... to generate additional configurations

$$\tilde{P}^{\mathbf{P}} = \frac{1}{(2\pi)^3} \int d^3X \exp\{-i(\tilde{\mathbf{P}} - \mathbf{P}) \cdot \mathbf{X}\}$$

PAV, VAP and Multiconfiguration

Projection After Variation (PAV)

- mean-field may break symmetries of Hamiltonian
- restore inversion, translational and rotational symmetry by projection on parity, linear and angular momentum

$$\tilde{P}^\pi = \frac{1}{2}(1 + \pi \tilde{\Pi})$$

$$\tilde{P}_{MK}^J = \frac{2J+1}{8\pi^2} \int d^3\Omega D_{MK}^J(\Omega) \tilde{R}(\Omega)$$

Variation After Projection (VAP)

- effect of projection can be large
- **Variation after Angular Momentum and Parity Projection** (VAP) for light nuclei
- combine VAP with **constraints** on **radius**, **dipole** moment, **quadrupole** moment, ... to generate additional configurations

$$\tilde{P}^{\mathbf{P}} = \frac{1}{(2\pi)^3} \int d^3X \exp\{-i(\tilde{\mathbf{P}} - \mathbf{P}) \cdot \mathbf{X}\}$$

Multiconfiguration Calculations

- **diagonalize** Hamiltonian in a set of projected intrinsic states

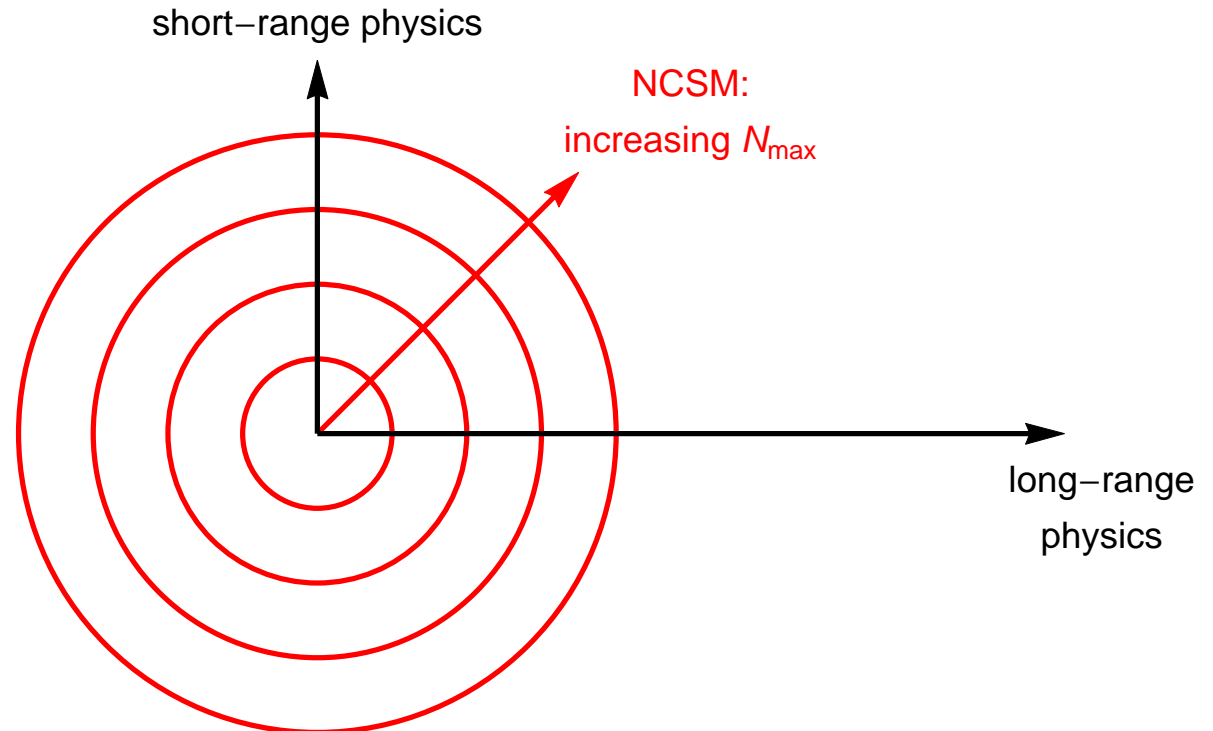
$$\left\{ |Q^{(a)}\rangle, \quad a = 1, \dots, N \right\}$$

$$\sum_{K'b} \langle Q^{(a)} | \tilde{H} \tilde{P}_{KK'}^{\pi} \tilde{P}^{\mathbf{P}=0} | Q^{(b)} \rangle \cdot c_{K'b}^\alpha =$$

$$E^{\pi\alpha} \sum_{K'b} \langle Q^{(a)} | \tilde{P}_{KK'}^{\pi} \tilde{P}^{\mathbf{P}=0} | Q^{(b)} \rangle \cdot c_{K'b}^\alpha$$

• FMD

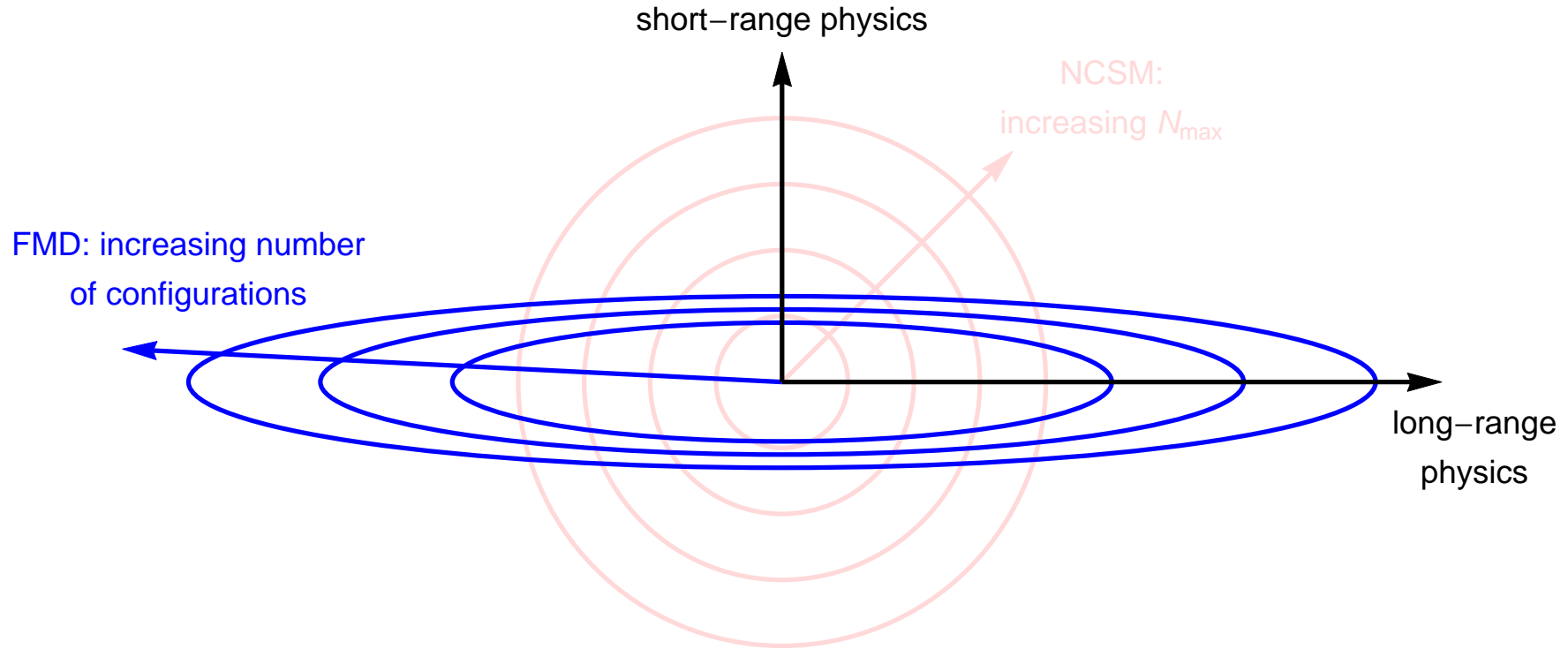
FMD vs NCSM model spaces



- NCSM allows good description of short-range physics, but long-range behavior suffers from harmonic oscillator asymptotics

• FMD

FMD vs NCSM model spaces



- NCSM allows good description of short-range physics, but long-range behavior suffers from harmonic oscillator asymptotics
- FMD allows to describe long-range physics by superposition of localized cluster configurations, but limited in description of short-range physics

Clustering and Localization



Localization and Kinetic Energy

- **Localization of center-of-mass wave function**
 - **Localization in the relative wave function due to clustering**
 - **Localization means large kinetic energy**
 - **Delocalization by angular momentum projection and configuration mixing lowers kinetic energy**
- ➡ Illustrate for ${}^8\text{Be} - {}^4\text{He}-{}^4\text{He}$ example
Volkov interaction – same width parameter a for all Gaussians

- Localization
- Center-of-Mass

- Slater determinants have a localized center-of-mass
- Center-of-mass wave function (in case of equal width parameters a)

$$\Psi_{\text{cm}}(\mathbf{X}) = \frac{1}{(\pi a_{\text{cm}})^{3/4}} \exp \left\{ -\frac{\mathbf{X}^2}{2a_{\text{cm}}} \right\}$$

with $a_{\text{cm}} = a/A$

- Kinetic energy of center-of-mass motion

$$\langle T_{\text{cm}} \rangle = \frac{1}{2Am} \frac{3}{2a_{\text{cm}}} = \frac{1}{2m} \frac{3}{2a}$$

$$|\Psi\rangle = |\Psi_{\text{intr}}\rangle \otimes |\Psi_{\text{cm}}\rangle$$

	⁴ He	$\min \langle H \rangle$	$\min \langle H - T_{\text{cm}} \rangle$
$\langle H - T_{\text{cm}} \rangle$	-25.42	-27.41	
$\langle T - T_{\text{cm}} \rangle$	36.76	49.14	
$\langle V \rangle$	-62.18	-76.54	
$\langle T_{\text{cm}} \rangle$	12.26	16.38	

	⁸ Be	$\min \langle H \rangle$	$\min \langle H - T_{\text{cm}} \rangle$
$\langle H - T_{\text{cm}} \rangle$	-44.05	-45.10	
$\langle T - T_{\text{cm}} \rangle$	102.62	117.62	
$\langle V \rangle$	-146.68	-162.72	
$\langle T_{\text{cm}} \rangle$	13.03	15.18	

- ➡ Minimizing $\langle H - T_{\text{cm}} \rangle$ corresponds to (approximate) variation after linear momentum projection
- ➡ Large effect on the wave function (at least for light nuclei)

- Localization

Relative Motion of Clusters

- GCM type Slater determinant – localized relative motion
- Relative wave function (in case of equal width parameters a) of two clusters at distance \mathbf{R}

$$\Psi_{\text{rel}}(\mathbf{r}) = \frac{1}{(\pi a_{\text{rel}})^{3/4}} \exp \left\{ -\frac{(\mathbf{r} - \mathbf{R})^2}{2a_{\text{rel}}} \right\}$$

with $a_{\text{rel}} = a/\mu_A$

- Kinetic energy of relative motion (at large distances)

$$\langle T_{\text{rel}} \rangle = \frac{1}{2\mu_A m} \frac{3}{2a_{\text{rel}}} = \frac{1}{2m} \frac{3}{2a}$$

$$|\Psi\rangle = \mathcal{A} \left\{ |\Psi_\alpha(-\frac{1}{2}\mathbf{R})\rangle \otimes |\Psi_\alpha(\frac{1}{2}\mathbf{R})\rangle \right\}$$

$$|\Psi_{\text{intr}}\rangle = \mathcal{A} \left\{ |\Psi_{\text{rel}}\rangle \otimes |\Phi_\alpha\rangle \otimes |\Phi_\alpha\rangle \right\}$$

$${}^8\text{Be} - \min \langle H - T_{\text{cm}} \rangle$$

	intrinsic	projected
$\langle H - T_{\text{cm}} \rangle$	-44.32	-51.01
$\langle T - T_{\text{cm}} \rangle$	131.05	126.48
$\langle V \rangle$	-175.37	-177.49
$\langle T_{\text{cm}} \rangle$	17.11	17.11

$${}^8\text{Be} - \min \langle 0^+ | H - T_{\text{cm}} | 0^+ \rangle$$

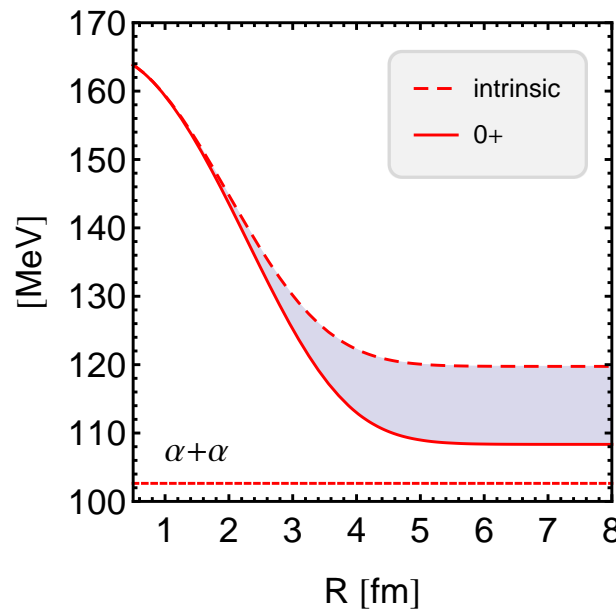
	intrinsic	projected
$\langle H - T_{\text{cm}} \rangle$	-31.77	-53.05
$\langle T - T_{\text{cm}} \rangle$	125.53	113.82
$\langle V \rangle$	-157.53	-166.87
$\langle T_{\text{cm}} \rangle$	17.11	17.11

➡ angular momentum projection delocalizes relative motion in two directions

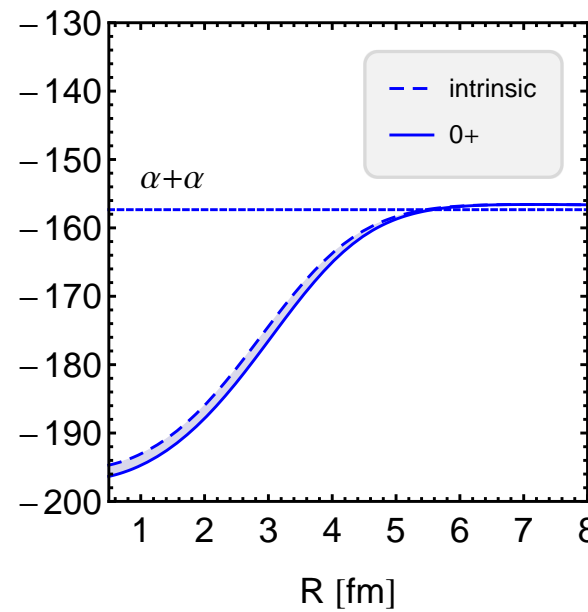
➡ delocalization in radial direction by configuration mixing

- Localization
- α - α Energy Surface

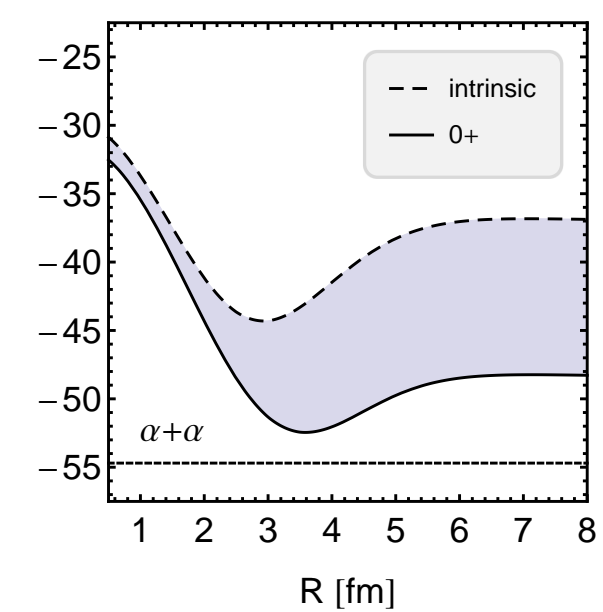
Kinetic Energy



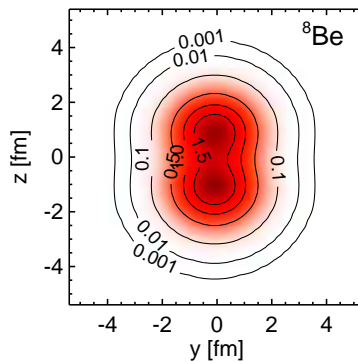
Potential Energy



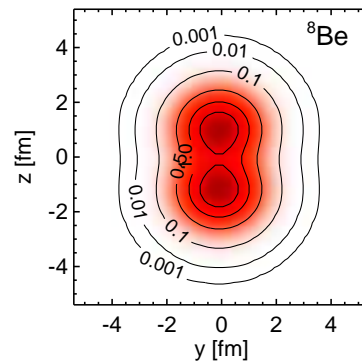
Total Energy



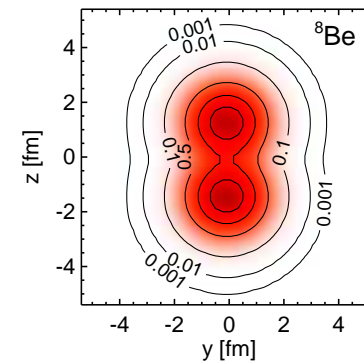
$R = 0.5\text{fm}$



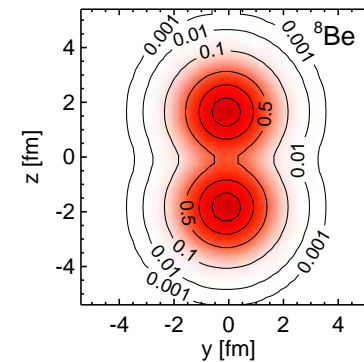
$R = 1.5\text{fm}$



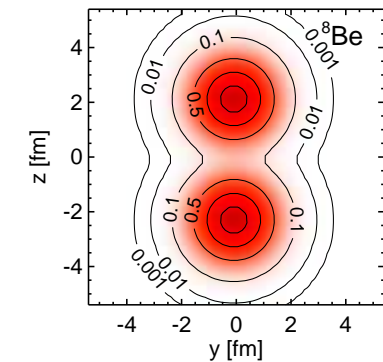
$R = 2.5\text{fm}$



$R = 3.5\text{fm}$



$R = 4.5\text{fm}$



Localization and Antisymmetrization



Compare THSR and GCM wave functions for ${}^8\text{Be}$

- **What is similar, what is different ?
RGM wave function**
- **What is the effect of Antisymmetrization ?
Define $\alpha\text{-}\alpha$ wave function by folding RGM wave function with square root of RGM norm kernel**
- **Localization or Delocalization ?
Probability Distribution**

- THSR vs GCM
- Wave functions

THSR wave function

Funaki *et al.*, Prog. Theor. Phys. 108, 297 (2002)

- spherical THSR wave function

$$\Phi_{\text{RGM}}(\mathbf{r}) = \exp \left\{ -\frac{r^2}{b^2 + \beta^2} \right\}$$

- prolate THSR wave function

$$\Phi_{\text{RGM}}(\mathbf{r}) = \exp \left\{ -\frac{r_x^2 + r_y^2}{b^2 + \beta_x^2} - \frac{r_z^2}{b^2 + \beta_z^2} \right\}$$

GCM wave function

- Brink-type cluster wave function

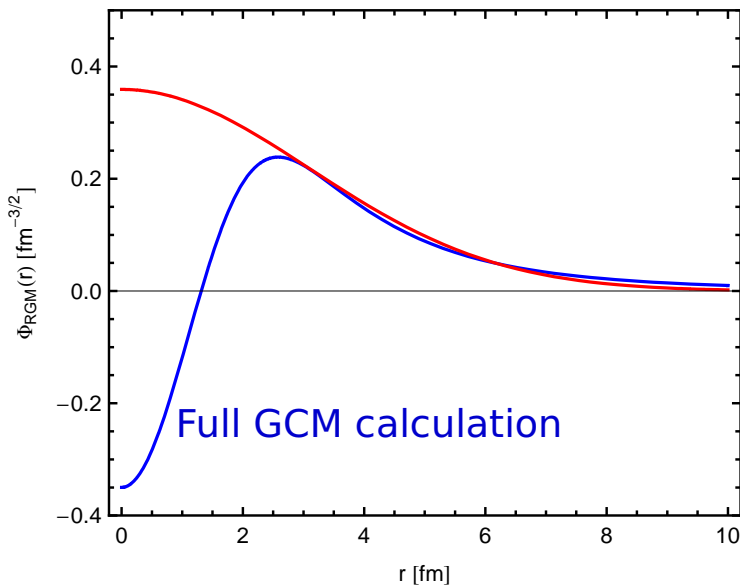
$$\Phi_{\text{RGM}}(\mathbf{r}) = \sum_i c_i \left(\frac{\mu_A}{\pi a} \right)^{3/4} \exp \left\{ -\mu_A \frac{(\mathbf{r} - \mathbf{R}_i)^2}{2a} \right\}$$

- GCM 1 config: $R = 3.5$ fm
- GCM 6 config: $R = \{1.5, 3.0, 4.5, 6.0, 7.5, 9.0\}$ fm
- GCM exact: $R = \{1.0, 2.0, \dots, 30.0\}$ fm

- THSR vs GCM

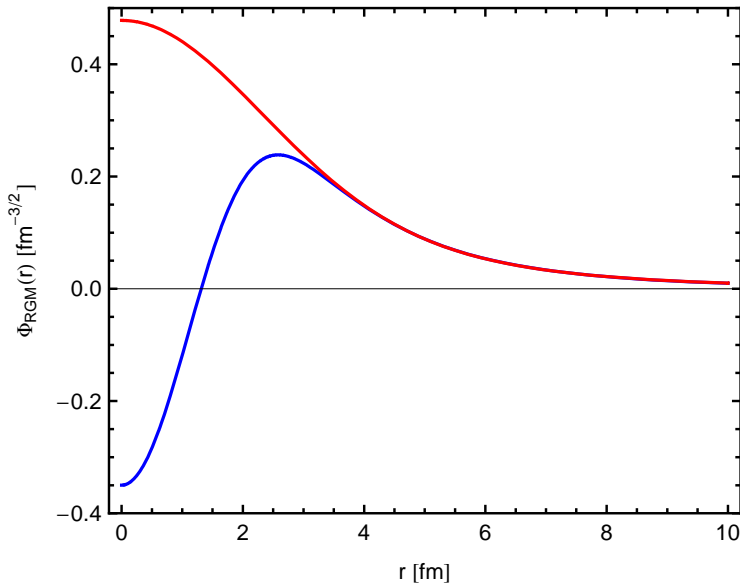
- RGM wave functions $\Phi_{\text{RGM}}(r)$

THSR spherical

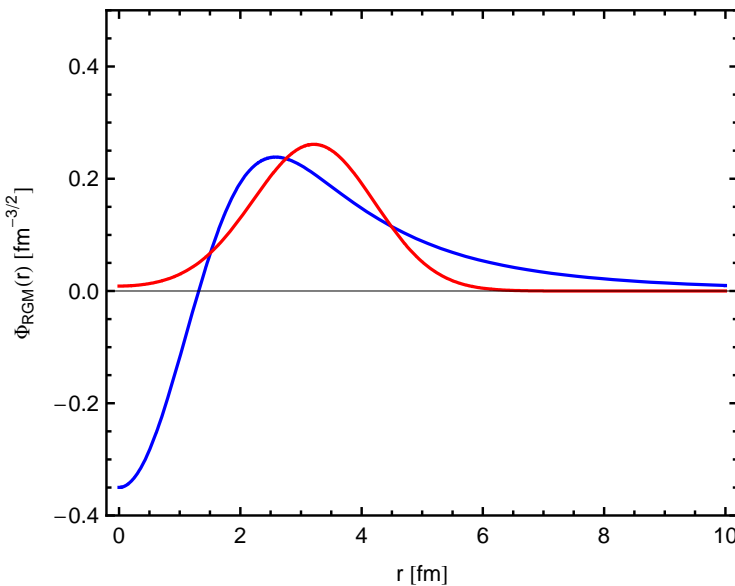


Full GCM calculation

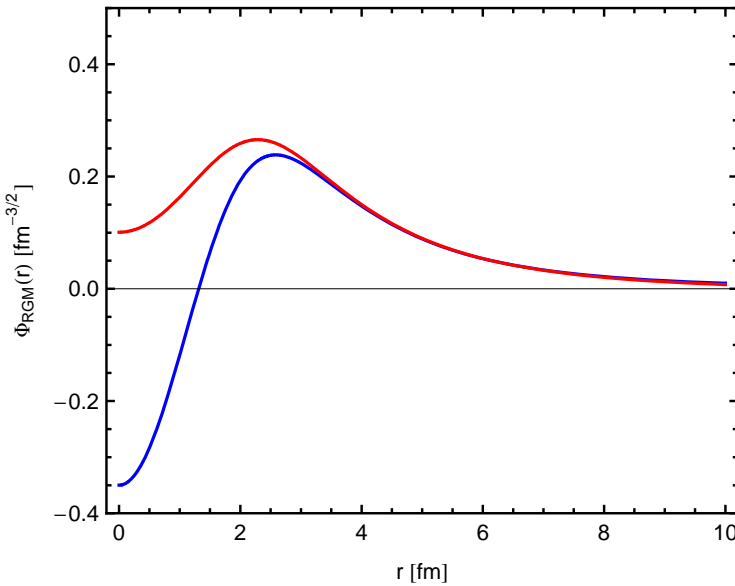
THSR prolate



GCM one config



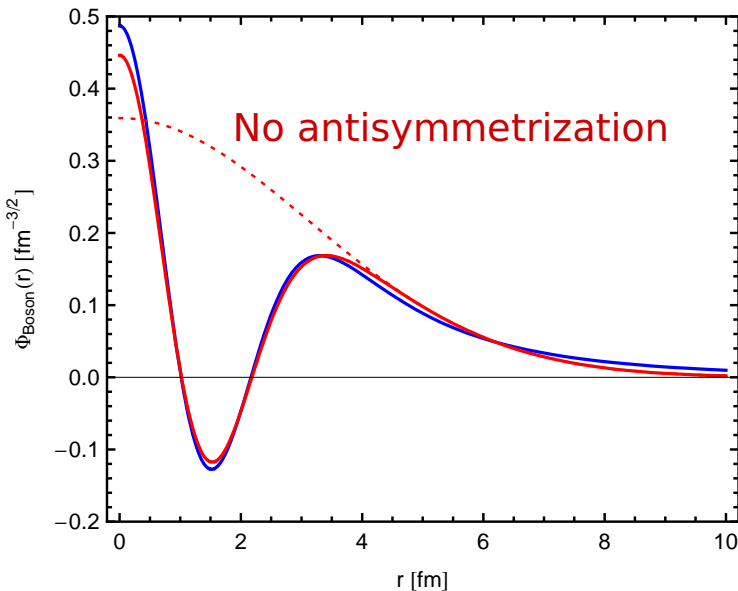
GCM six configs



- THSR vs GCM

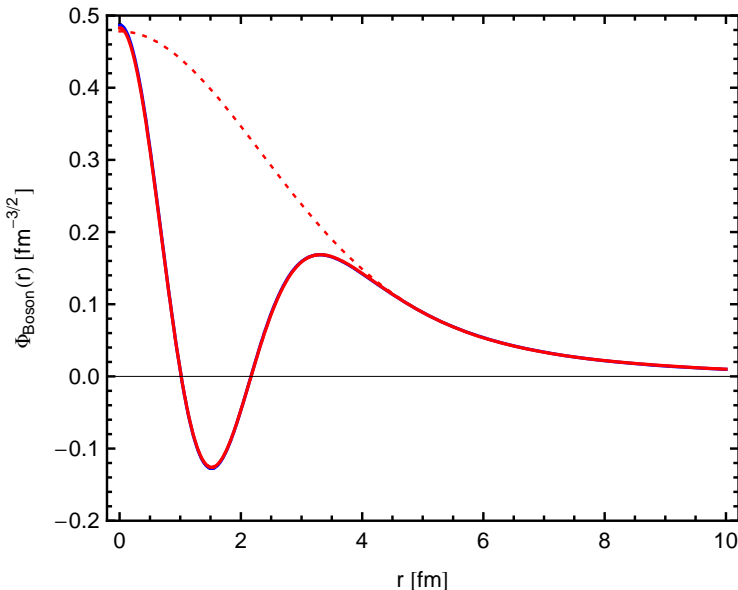
- $\alpha\text{-}\alpha$ wave functions $\Phi_{\alpha\text{-}\alpha}(r) = \int dr' r'^2 N^{1/2}(r, r') \Phi_{\text{RGM}}(r')$

THSR spherical

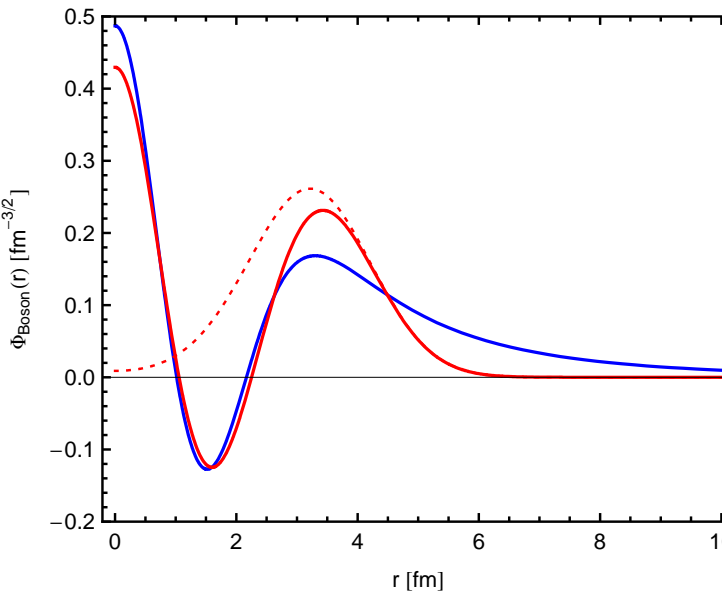


No antisymmetrization

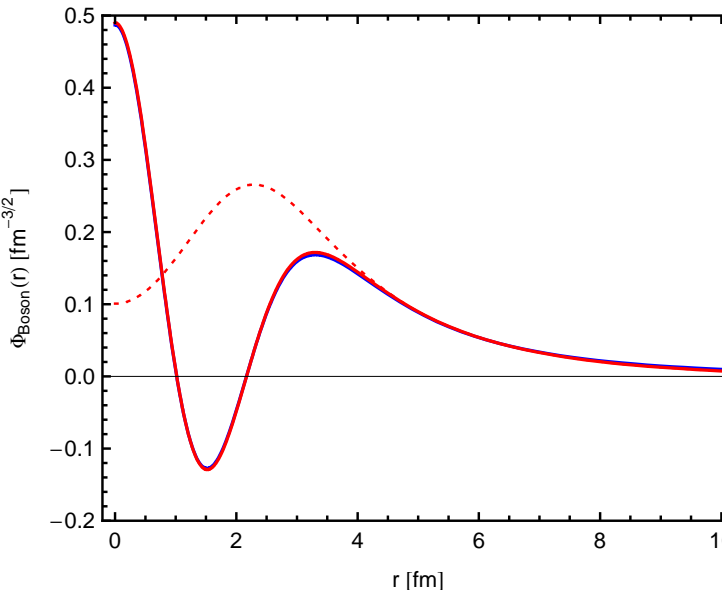
THSR prolate



GCM one config



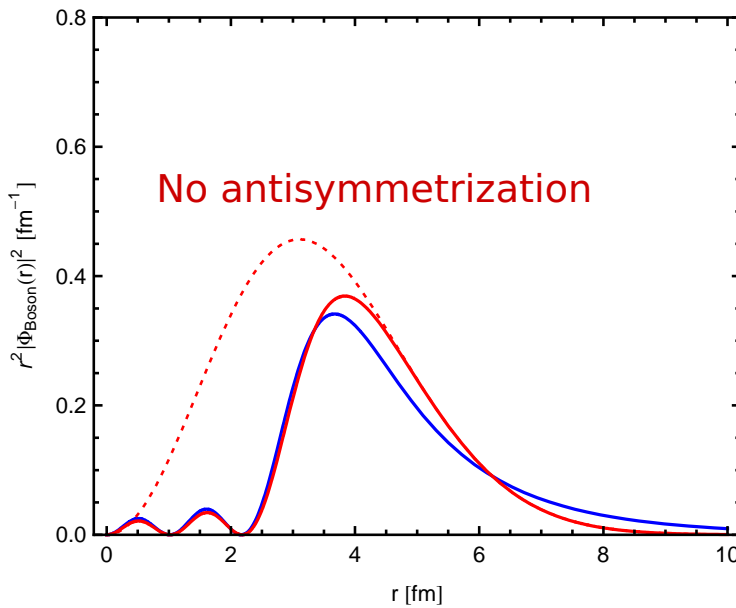
GCM six configs



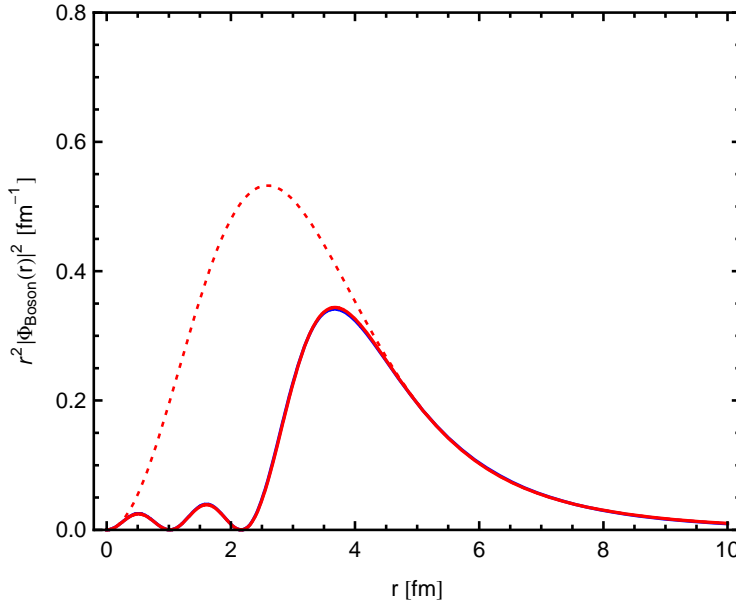
- THSR vs GCM

- Probability Density $r^2 |\Phi_{\alpha-\alpha}(r)|^2$

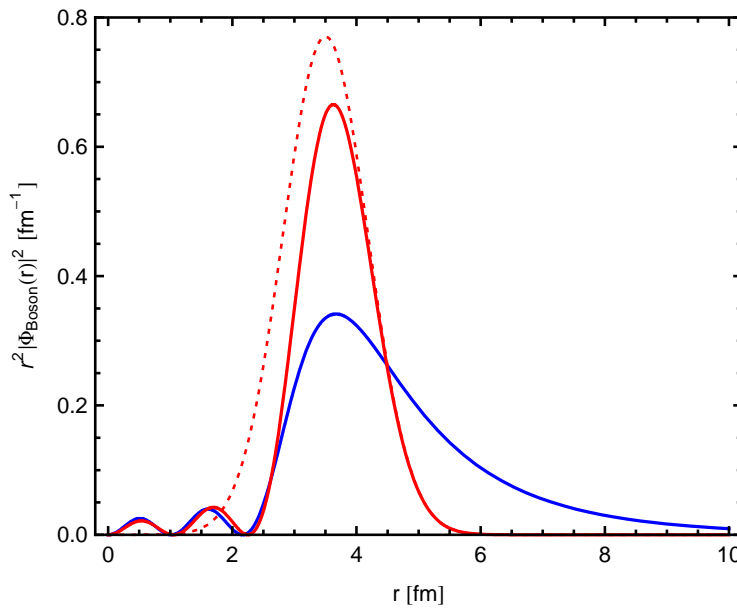
THSR spherical



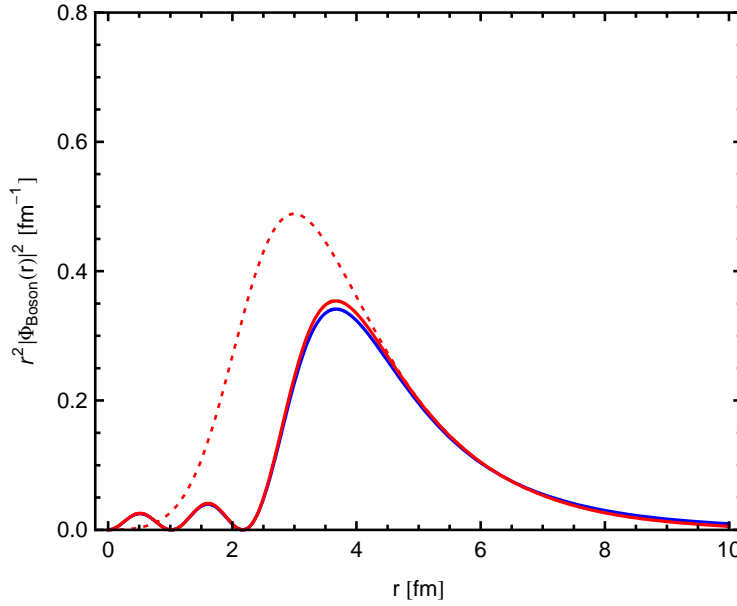
THSR prolate



GCM one config



GCM six configs



- THSR vs GCM
- Conclusions

- THSR is a great variational wave function
 - deformed THSR wave function allows for non-Gaussian asymptotics
 - short-range behavior of RGM wave function unimportant because of antisymmetrization
- ➡ α - α wave function “localized” outside range of antisymmetrization but “delocalized” in the tail
- ➡ Only α - α wave functions (including antisymmetrization and RGM norm kernel) can be compared in a meaningful way

$^3\text{He}(\alpha, \gamma)^7\text{Be}$ radiative capture

one of the key reactions in the solar pp-chains



Effective Nucleon-Nucleon interaction:

UCOM(SRG) $\alpha = 0.20 \text{ fm}^4 - \lambda \approx 1.5 \text{ fm}^{-1}$

Many-Body Approach:

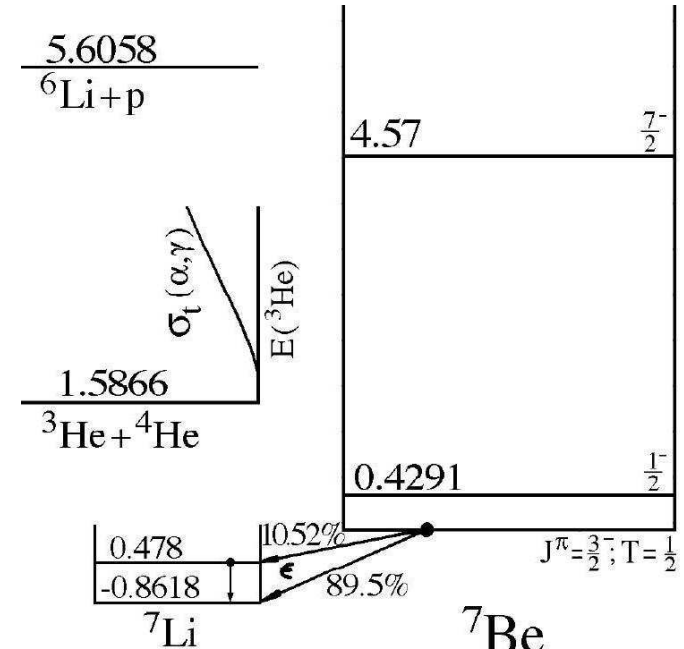
Fermionic Molecular Dynamics

- Internal region: VAP configurations with radius constraint
- External region: Brink-type cluster configurations
- Matching to Coulomb solutions: Microscopic R -matrix method

Results:

- ^7Be bound and scattering states
- Astrophysical S-factor

T. Neff, Phys. Rev. Lett. **106**, 042502 (2011)



- ${}^3\text{He}(\alpha, \gamma){}^7\text{Be}$
- FMD model space

Frozen configurations

- 15 antisymmetrized wave function built with ${}^4\text{He}$ and ${}^3\text{He}$ FMD clusters up to channel radius $a=12$ fm

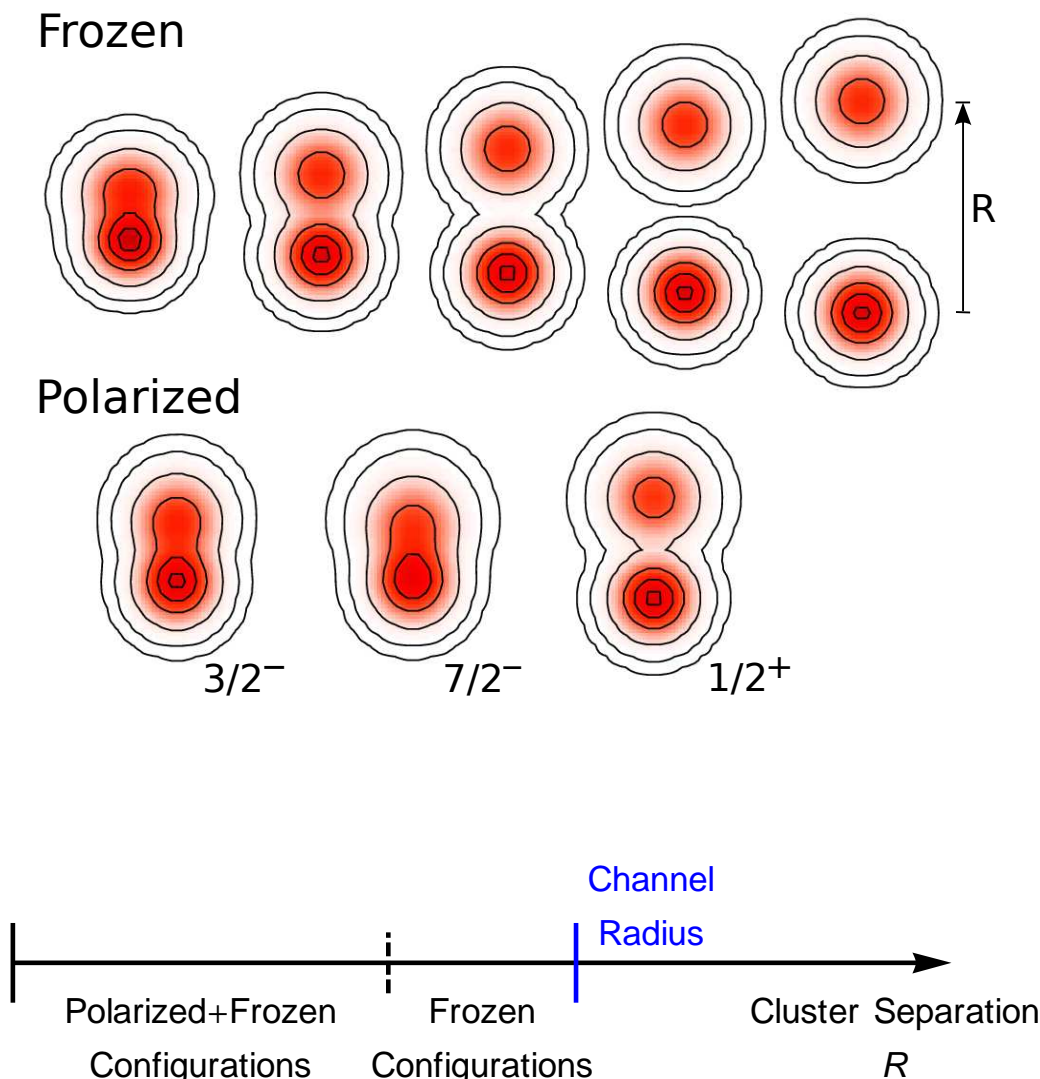
Polarized configurations

- 30 FMD wave functions obtained by VAP on $1/2^-$, $3/2^-$, $5/2^-$, $7/2^-$ and $1/2^+$, $3/2^+$ and $5/2^+$ combined with radius constraint in the interaction region

Boundary conditions

- Match relative motion of clusters at channel radius to Whittaker/Coulomb functions with the **microscopic R-matrix** method of the Brussels group

D. Baye, P.-H. Heenen, P. Descouvemont



- $^3\text{He}(\alpha, \gamma)^7\text{Be}$

p -wave Bound and Scattering States

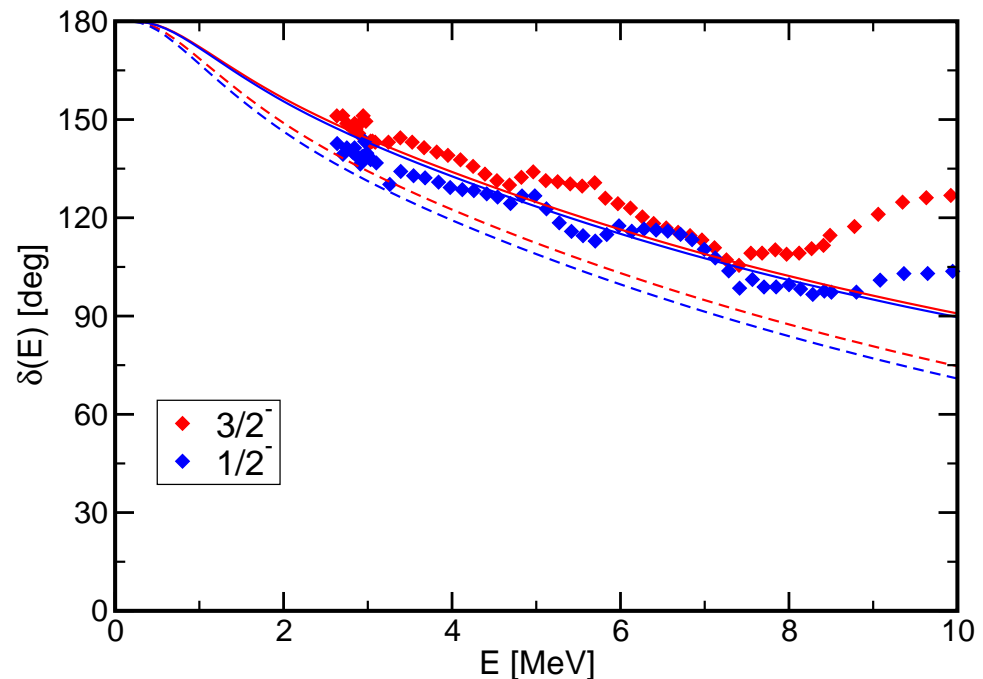
Bound states

		Experiment	FMD
^7Be	$E_{3/2^-}$	-1.59 MeV	-1.49 MeV
	$E_{1/2^-}$	-1.15 MeV	-1.31 MeV
	r_{ch}	2.647(17) fm	2.67 fm
	Q	–	-6.83 e fm ²
^7Li	$E_{3/2^-}$	-2.467 MeV	-2.39 MeV
	$E_{1/2^-}$	-1.989 MeV	-2.17 MeV
	r_{ch}	2.444(43) fm	2.46 fm
	Q	-4.00(3) e fm ²	-3.91 e fm ²

- centroid of bound state energies well described if polarized configurations included
- tail of wave functions tested by charge radii and quadrupole moments

Phase shift analysis:

Spiger and Tombrello, PR **163**, 964 (1967)

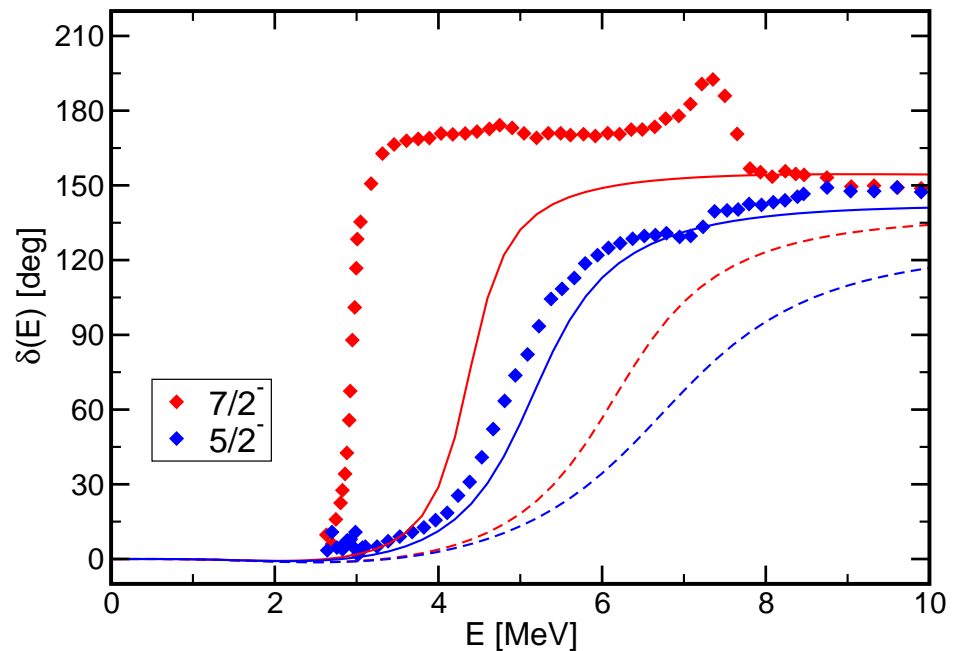
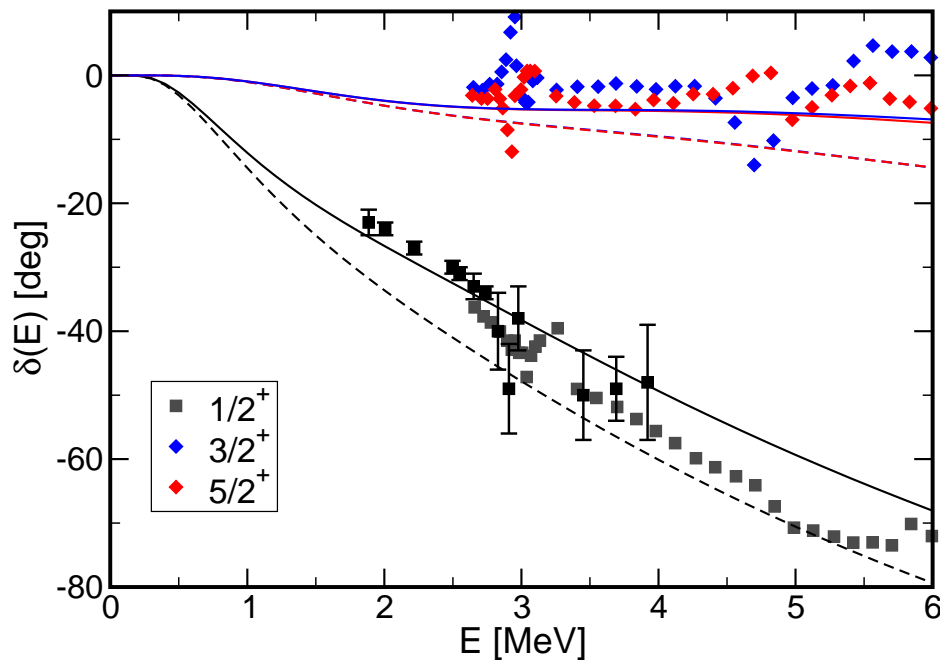


dashed lines – frozen configurations only
 solid lines – polarized configurations in interaction region included

- Scattering phase shifts well described, polarization effects important

- $^3\text{He}(\alpha, \gamma)^7\text{Be}$

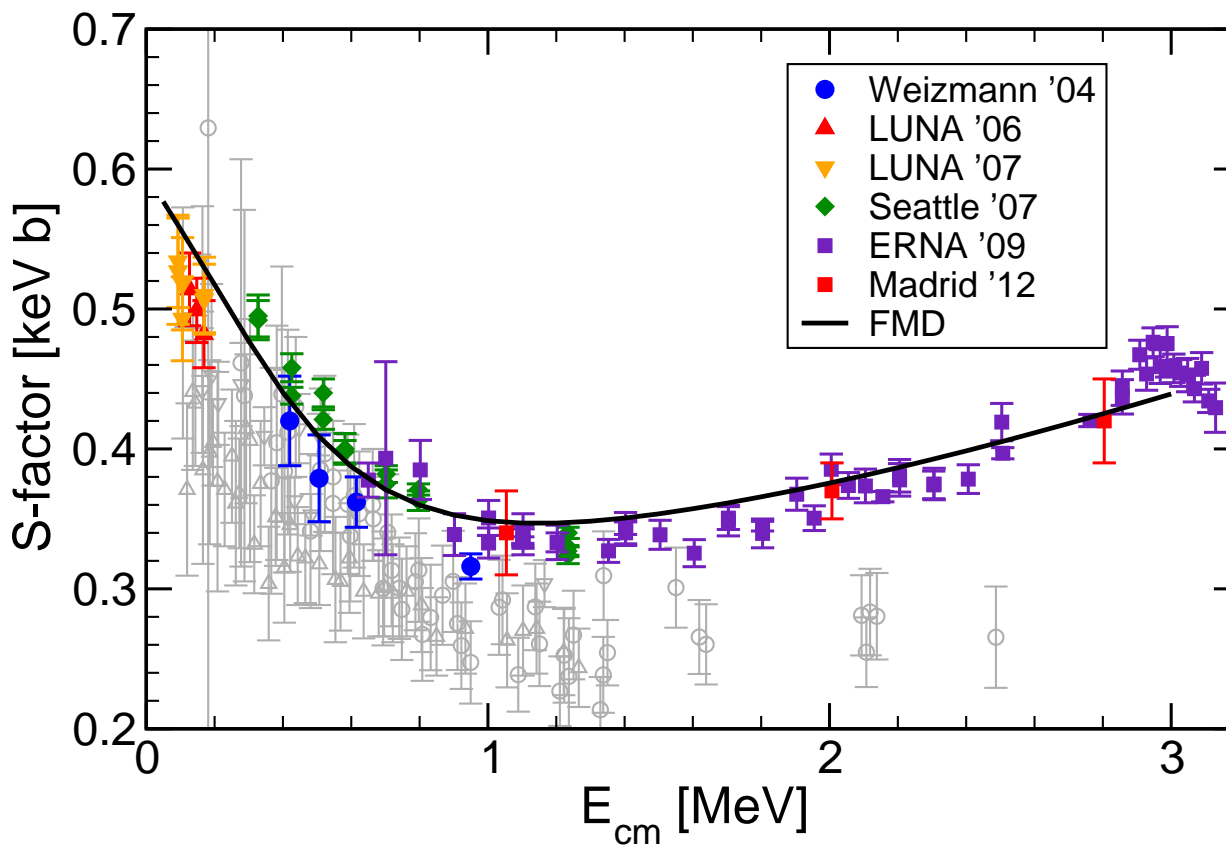
s-, d- and f-wave Scattering States



dashed lines – frozen configurations only – solid lines – FMD configurations in interaction region included

- polarization effects important
- *s-* and *d*-wave scattering phase shifts well described
- $7/2^-$ resonance too high, $5/2^-$ resonance roughly right, consistent with no-core shell model calculations

• $^3\text{He}(\alpha, \gamma)^7\text{Be}$
 • S-Factor



S-factor:

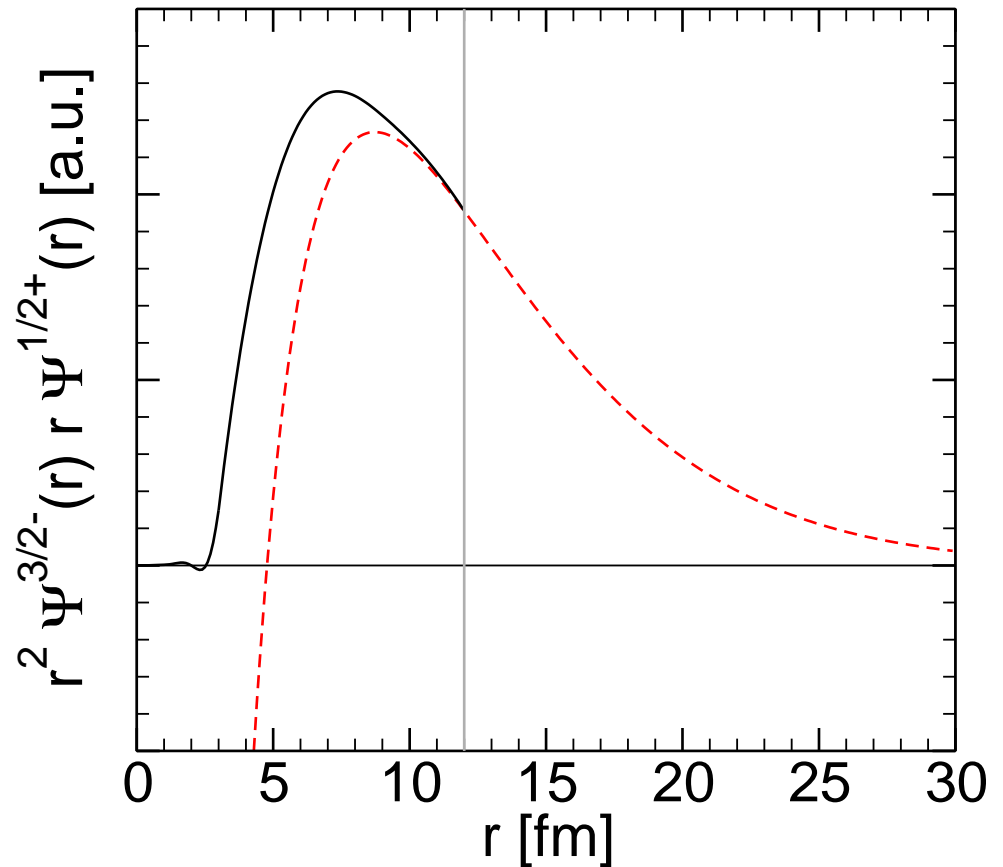
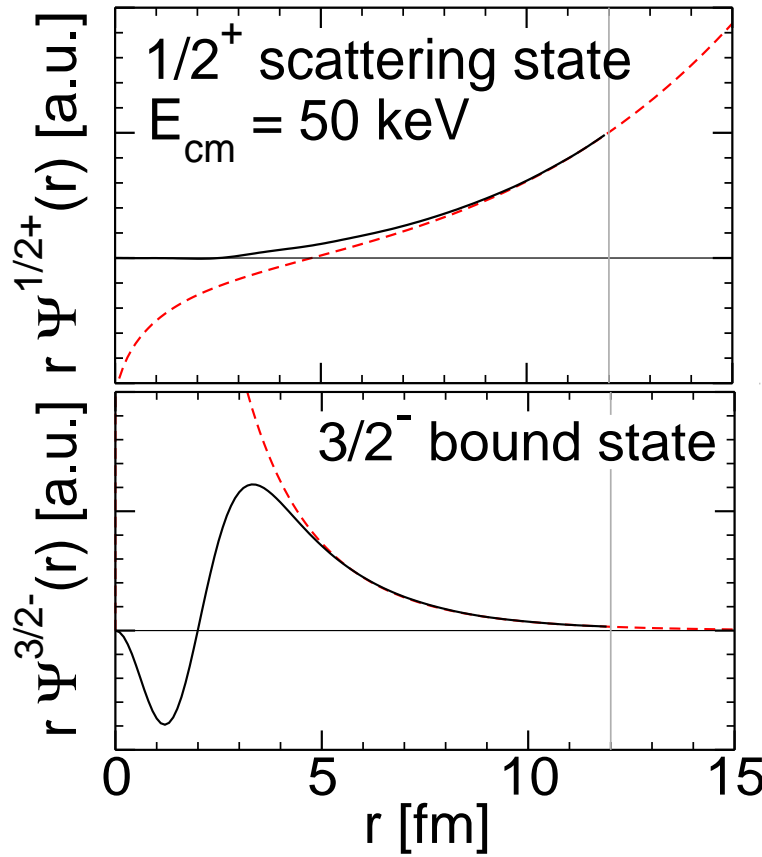
$$S(E) = \sigma(E)E \exp\{2\pi\eta\}$$

$$\eta = \frac{\mu Z_1 Z_2 e^2}{k}$$

Nara Singh *et al.*, PRL **93**, 262503 (2004)
 Bemmerer *et al.*, PRL **97**, 122502 (2006)
 Confortola *et al.*, PRC **75**, 065803 (2007)
 Brown *et al.*, PRC **76**, 055801 (2007)
 Di Leva *et al.*, PRL **102**, 232502 (2009)
 Carmona-Gallardo *et al.*,
 PRC **86**, 032801(R) (2012)

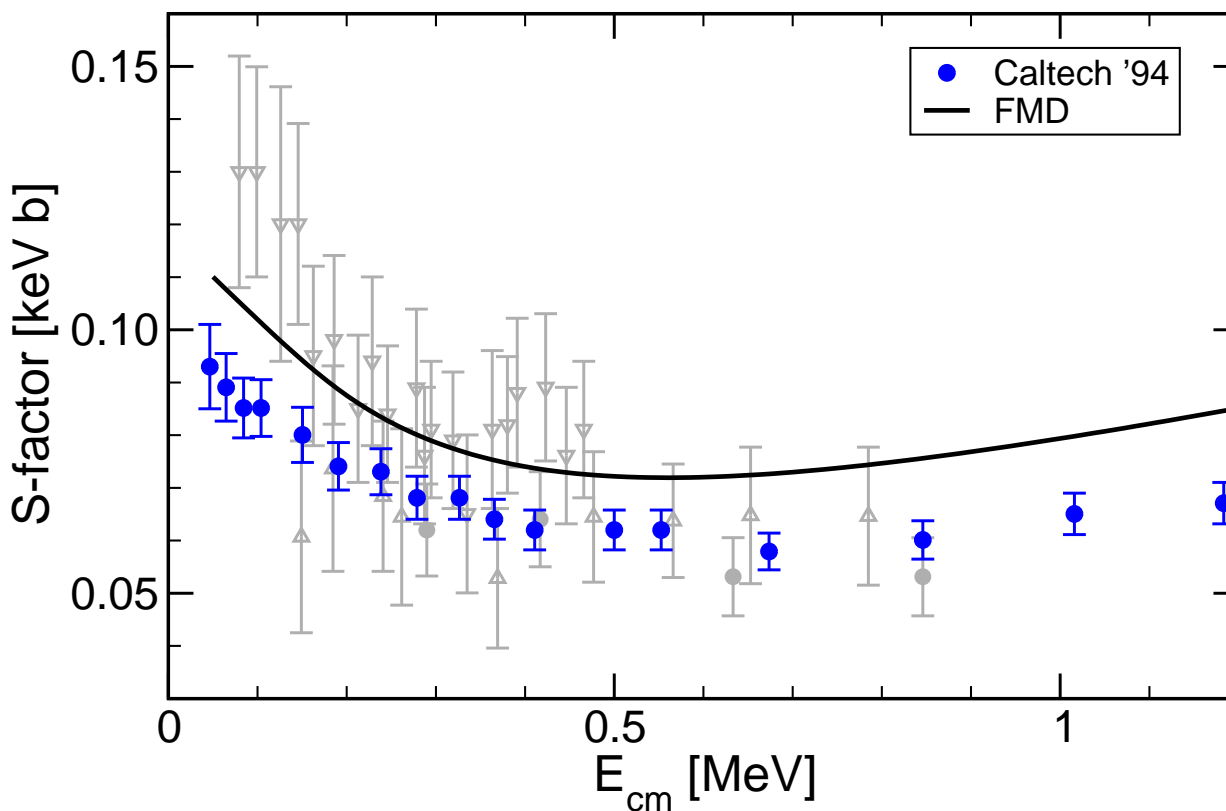
- dipole transitions from $1/2^+$, $3/2^+$, $5/2^+$ scattering states into $3/2^-$, $1/2^-$ bound states
- ➔ FMD is the only model that describes well the energy dependence and normalization of new high quality data
- ➔ fully microscopic calculation, bound and scattering states are described consistently

Overlap Functions and Dipole Matrixelements



- Overlap functions from projection on RGM-cluster states
- Coulomb and Whittaker functions matched at channel radius $a=12$ fm
- Dipole matrix elements calculated from overlap functions reproduce full calculation within 2%
- cross section depends significantly on internal part of wave function, description as an “external” capture is too simplified

● $^3\text{H}(\alpha, \gamma)^7\text{Li}$
● **S-Factor**



S-factor:

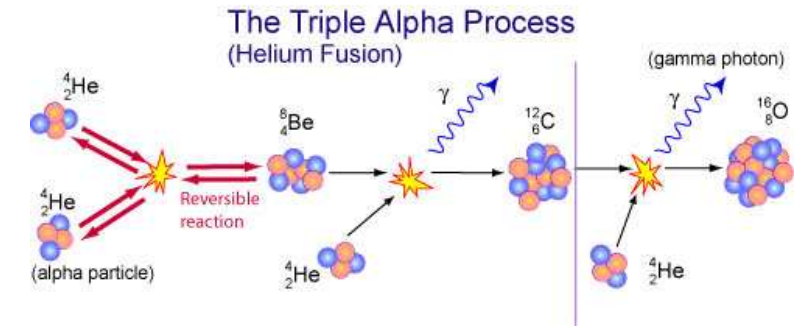
$$S(E) = \sigma(E)E \exp\{2\pi\eta\}$$

$$\eta = \frac{\mu Z_1 Z_2 e^2}{k}$$

Brune *et al.*, PRC **50**, 2205 (1994)

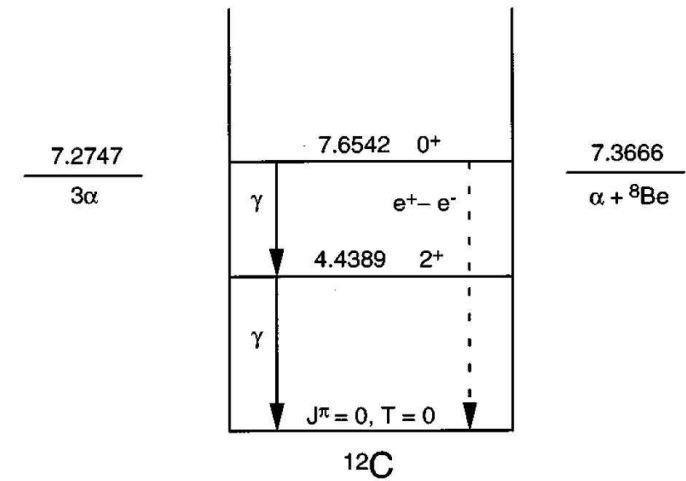
- isospin mirror reaction of $^3\text{He}(\alpha, \gamma)^7\text{Be}$
- ^7Li bound state properties and phase shifts well described
- ➡ FMD calculation describes energy dependence of Brune *et al.* data but cross section is larger by about 15%

Cluster States in ^{12}C



Astrophysical Motivation

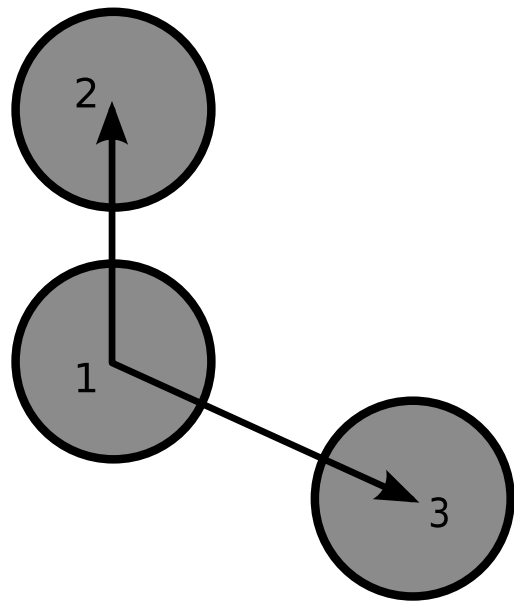
- Helium burning:
triple alpha-reaction



Structure

- Is the Hoyle state a pure α -cluster state ?
- Other excited 0^+ and 2^+ states
- Compare FMD results to microscopic α -cluster model
- Intrinsic structure from two-body densities
- Analyze wave functions in harmonic oscillator basis

- Cluster States in ^{12}C
- Microscopic α -Cluster Model



$$R_{12} = (2, 4, \dots, 10) \text{ fm}$$

$$R_{13} = (2, 4, \dots, 10) \text{ fm}$$

$$\cos(\theta) = (1.0, 0.8, \dots, -1.0)$$

alltogether 165 configurations

Basis States

- describe Hoyle State as a system of 3 ^4He nuclei

$$|\Psi_{3\alpha}(\mathbf{R}_1, \mathbf{R}_2, \mathbf{R}_3); JMK\pi\rangle = P_{MK}^J P^\pi \mathcal{A} \{ |\psi_\alpha(\mathbf{R}_1)\rangle \otimes |\psi_\alpha(\mathbf{R}_2)\rangle \otimes |\psi_\alpha(\mathbf{R}_3)\rangle \}$$

Volkov Interaction

- simple central interaction
- parameters adjusted to give reasonable α binding energy and radius, $\alpha - \alpha$ scattering data, adjusted to reproduce ^{12}C ground state energy
- ✗ only reasonable for ^4He , ^8Be and ^{12}C nuclei

'BEC' wave functions

- interpretation of the Hoyle state as a Bose-Einstein Condensate of α -particles by Funaki, Tohsaki, Horiuchi, Schuck, Röpke
- same interaction and α -cluster parameters used

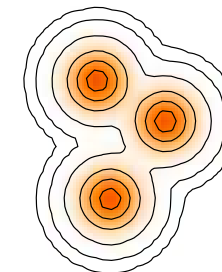
Kamimura, Nuc. Phys. **A351** (1981) 456

Funaki et al., Phys. Rev. C **67** (2003) 051306(R)

- Cluster States in ^{12}C
- FMD

Basis States

- 20 FMD states obtained in Variation after Projection on 0^+ and 2^+ with constraints on the radius
- 42 FMD states obtained in Variation after Projection on parity with constraints on radius and quadrupole deformation
- 165 α -cluster configurations
- projected on angular momentum and linear momentum

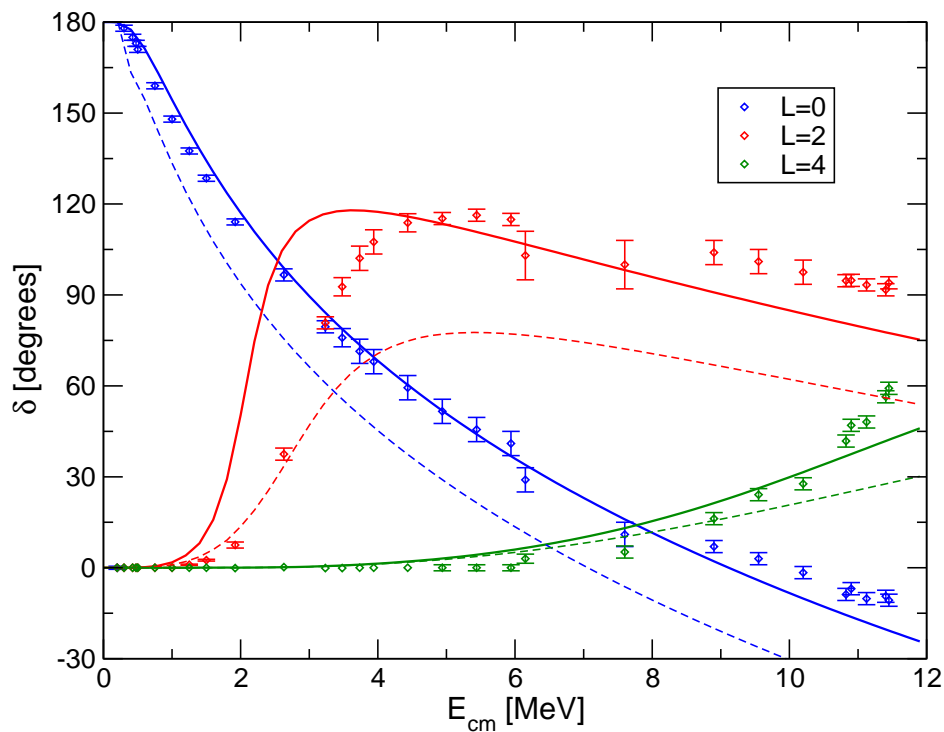


Interaction

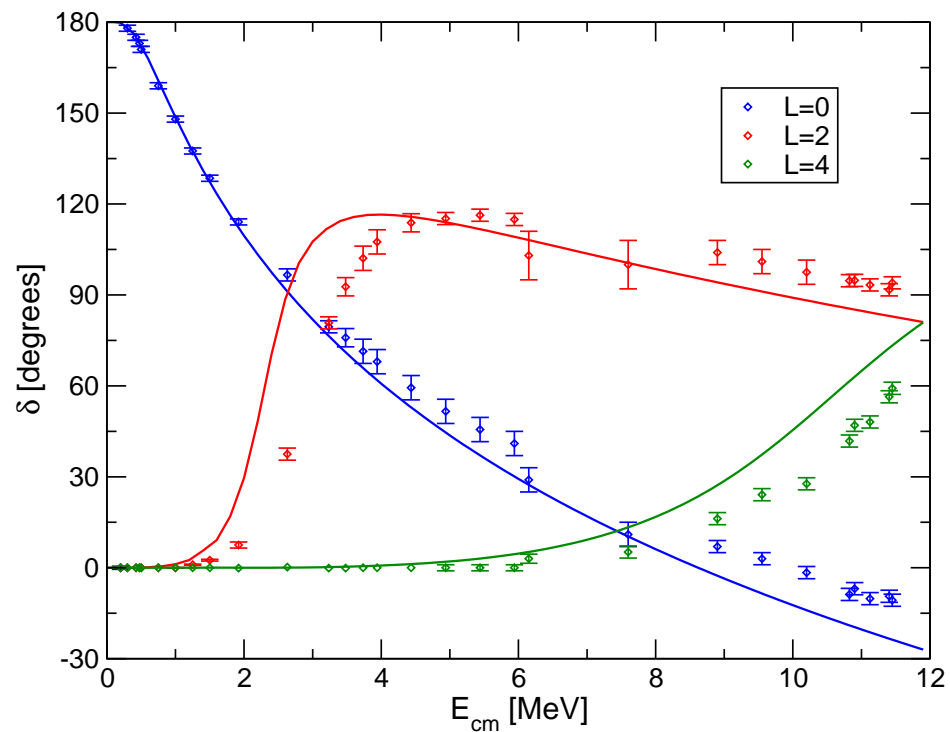
- UCOM interaction ($I_9=0.30 \text{ fm}^3$ with phenomenological two-body correction term (momentum-dependent central and spin-orbit) fitted to doubly-magic nuclei)
- not tuned for α - α scattering or ^{12}C properties

- Cluster States in ^{12}C
- α - α Phaseshifts

FMD



Cluster Model

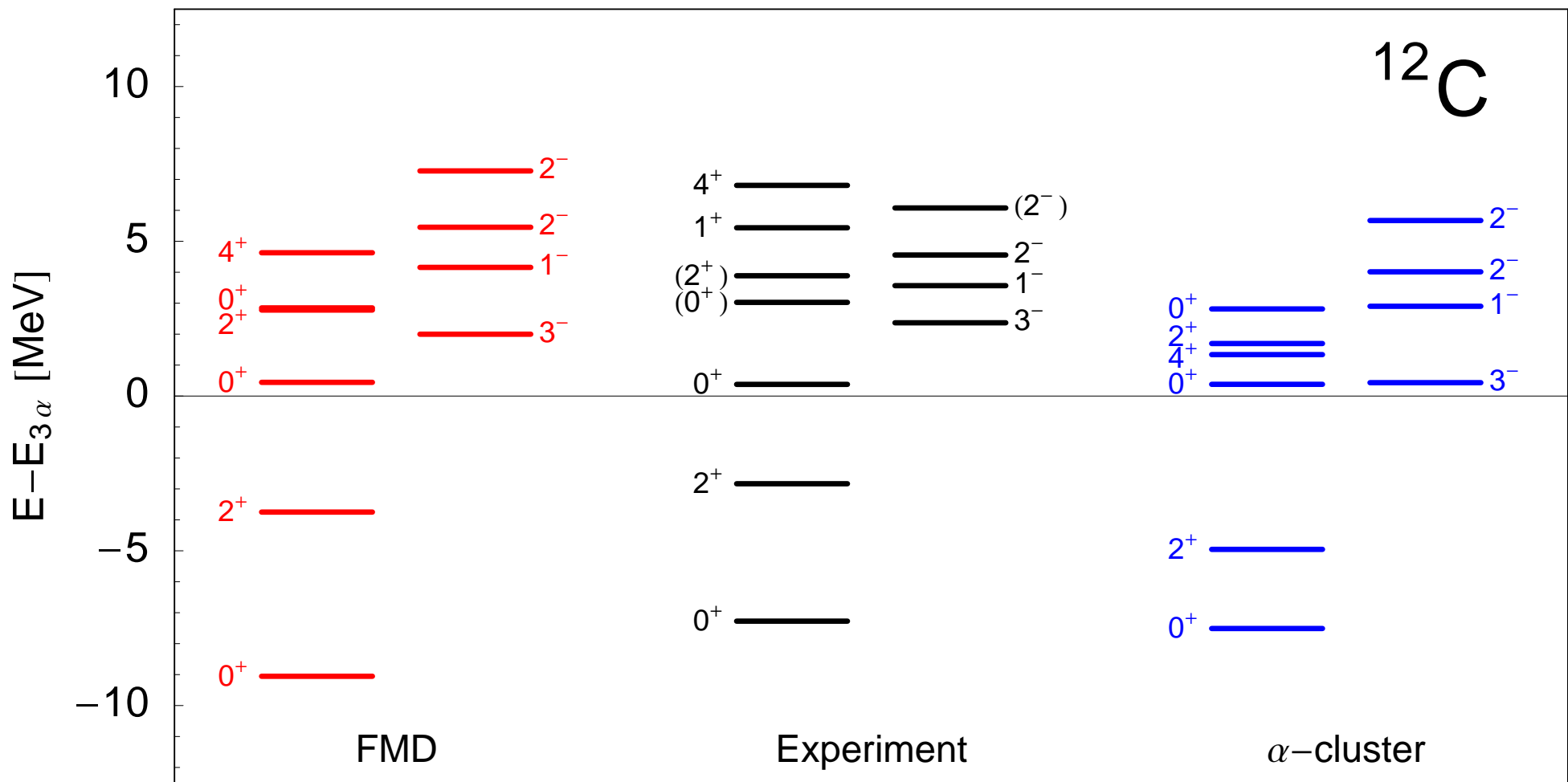


- Phaseshifts calculated with cluster configurations only (dashed lines)
- Phaseshifts calculated with additional FMD VAP configurations in the interaction region (solid lines)

- only cluster configurations included

➡ similar quality for description of α - α -scattering

- Cluster States in ^{12}C
- Comparison



- Cluster States in ^{12}C
- Comparison

	Exp ¹	Exp ²	FMD	α -cluster	'BEC' ³
$E(0^+_1)$	-92.16		-92.64	-89.56	-89.52
$E^*(2^+_1)$	4.44		5.31	2.56	2.81
$E(3\alpha)$	-84.89		-83.59	-82.05	-82.05
$E(0^+_2) - E(3\alpha)$	0.38		0.43	0.38	0.26
$E(0^+_3) - E(3\alpha)$	(3.0)	2.7(3)	2.84	2.81	
$E(2^+_2) - E(3\alpha)$	(3.89)	2.76(11)	2.77	1.70	
$r_{\text{charge}}(0^+_1)$	2.47(2)		2.53	2.54	
$r(0^+_1)$			2.39	2.40	2.40
$r(0^+_2)$			3.38	3.71	3.83
$r(0^+_3)$			4.62	4.75	
$r(2^+_1)$			2.50	2.37	2.38
$r(2^+_2)$			4.43	4.02	
$M(E0, 0^+_1 \rightarrow 0^+_2)$	5.4(2)		6.53	6.52	6.45
$B(E2, 2^+_1 \rightarrow 0^+_1)$	7.6(4)		8.69	9.16	
$B(E2, 2^+_1 \rightarrow 0^+_2)$	2.6(4)		3.83	0.84	
$B(E2, 2^+_2 \rightarrow 0^+_1)$		0.73(13)	0.46	1.99	

experimental situation for 0^+_3 and 2^+_2 states still unsettled (?)

2^+_2 resonance at 1.8 MeV above threshold included in NACRE compilation

¹ Ajzenberg-Selove, Nuc. Phys. **A506**, 1 (1990)

² Itoh et al., Nuc. Phys. **A738**, 268 (2004), Zimmermann et al., Phys. Rev. Lett. **110**, 152502 (2013)

³ Funaki et al., Phys. Rev. C **67**, 051306(R) (2003)

- Cluster States in ^{12}C
- Comparison

	Exp ¹	Exp ²	FMD	α -cluster	'BEC' ³
$E(0^+_1)$	-92.16		-92.64	-89.56	-89.52
$E^*(2^+_1)$	4.44		5.31	2.56	2.81
$E(3\alpha)$	-84.89		-83.59	-82.05	-82.05
$E(0^+_2) - E(3\alpha)$	0.38		0.43	0.38	0.26
$E(0^+_3) - E(3\alpha)$	(3.0)	2.7(3)	2.84	2.81	
$E(2^+_2) - E(3\alpha)$	(3.89)	2.76(11)	2.77	1.70	
$r_{\text{charge}}(0^+_1)$	2.47(2)		2.53	2.54	
$r(0^+_1)$			2.39	2.40	2.40
$r(0^+_2)$			3.38	3.71	3.83
$r(0^+_3)$			4.62	4.75	
$r(2^+_1)$			2.50	2.37	2.38
$r(2^+_2)$			4.43	4.02	
$M(E0, 0^+_1 \rightarrow 0^+_2)$	5.4(2)		6.53	6.52	6.45
$B(E2, 2^+_1 \rightarrow 0^+_1)$	7.6(4)		8.69	9.16	
$B(E2, 2^+_1 \rightarrow 0^+_2)$	2.6(4)		3.83	0.84	
$B(E2, 2^+_2 \rightarrow 0^+_1)$		0.73(13)	0.46	1.99	

experimental situation for 0^+_3 and 2^+_2 states still unsettled (?)

2^+_2 resonance at 1.8 MeV above threshold included in NACRE compilation

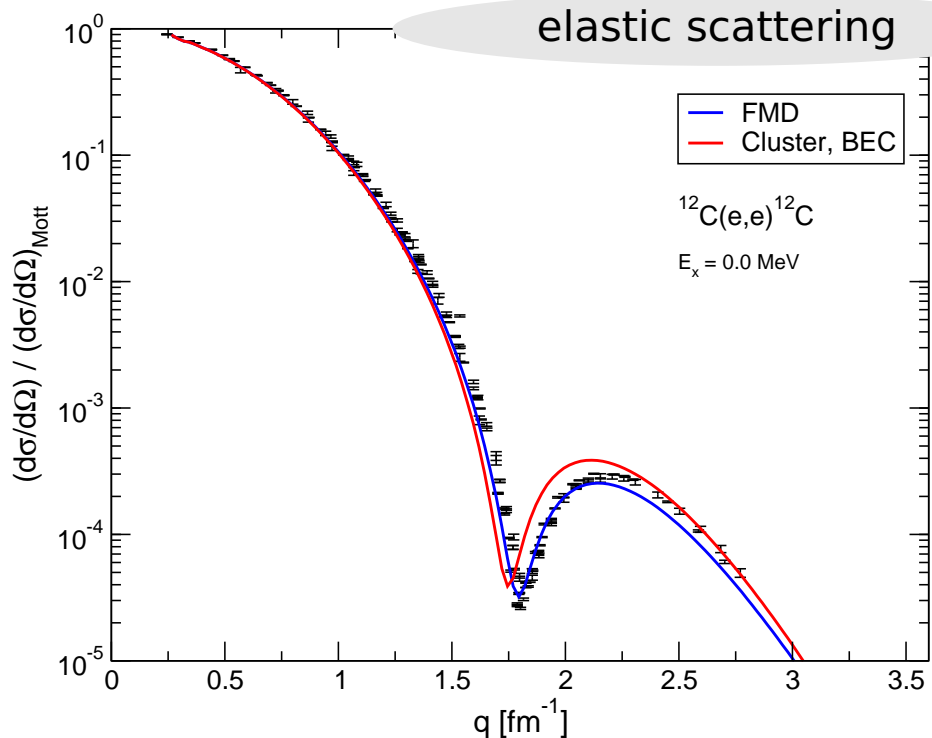
calculated in bound state approximation

¹ Ajzenberg-Selove, Nuc. Phys. **A506**, 1 (1990)

² Itoh et al., Nuc. Phys. **A738**, 268 (2004), Zimmermann et al., Phys. Rev. Lett. **110**, 152502 (2013)

³ Funaki et al., Phys. Rev. C **67**, 051306(R) (2003)

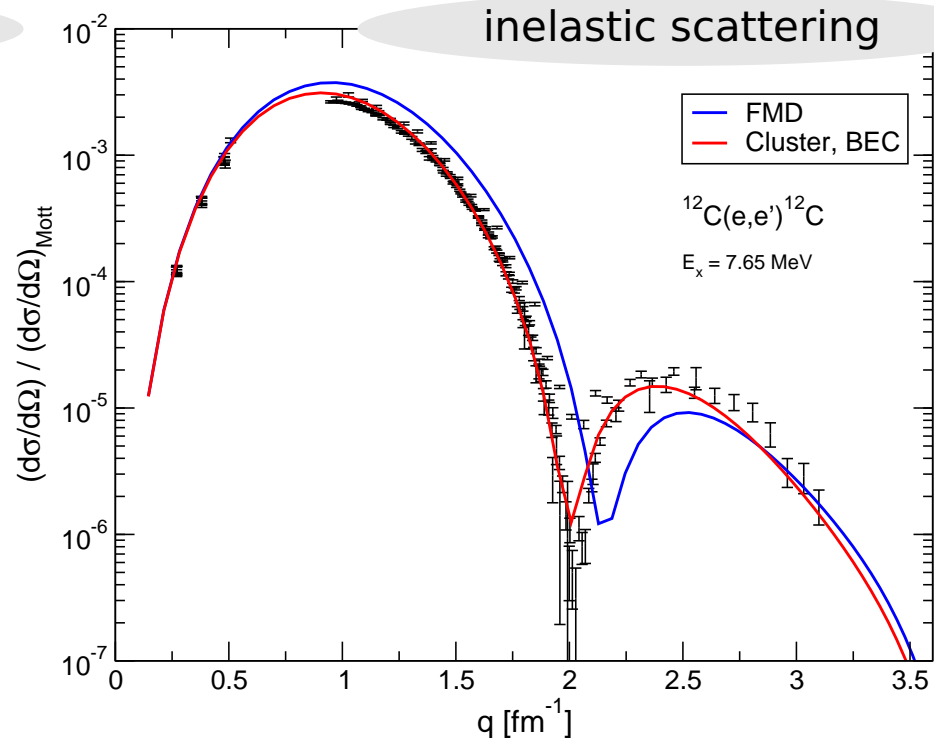
- Cluster States in ^{12}C
- Electron Scattering Data



elastic scattering

FMD
Cluster, BEC

$^{12}\text{C}(e,e)^{12}\text{C}$
 $E_x = 0.0 \text{ MeV}$



inelastic scattering

FMD
Cluster, BEC

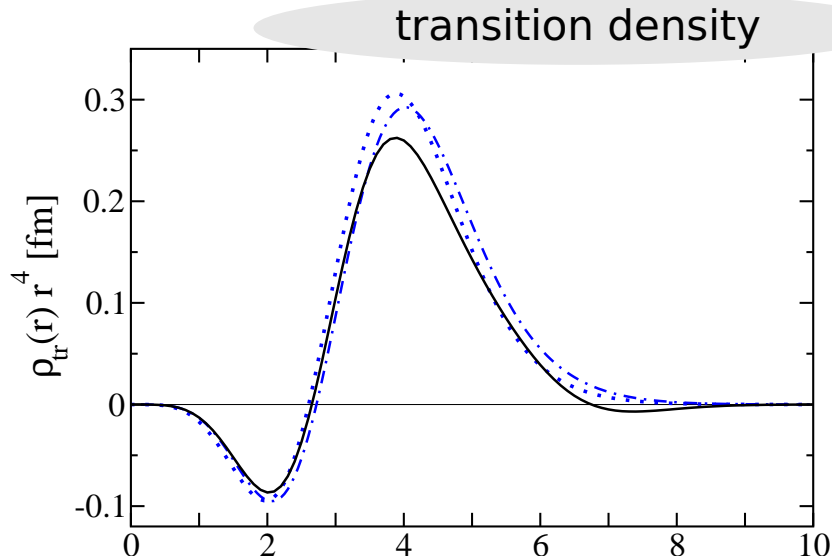
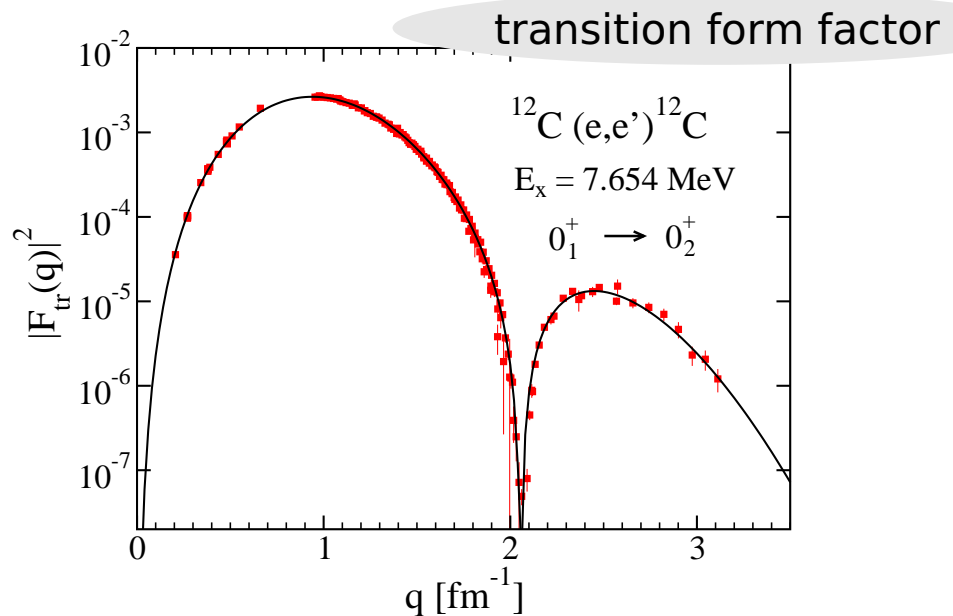
$^{12}\text{C}(e,e')^{12}\text{C}$
 $E_x = 7.65 \text{ MeV}$

- compare with precise electron scattering data up to high momenta in Distorted Wave Born Approximation
- use intrinsic density

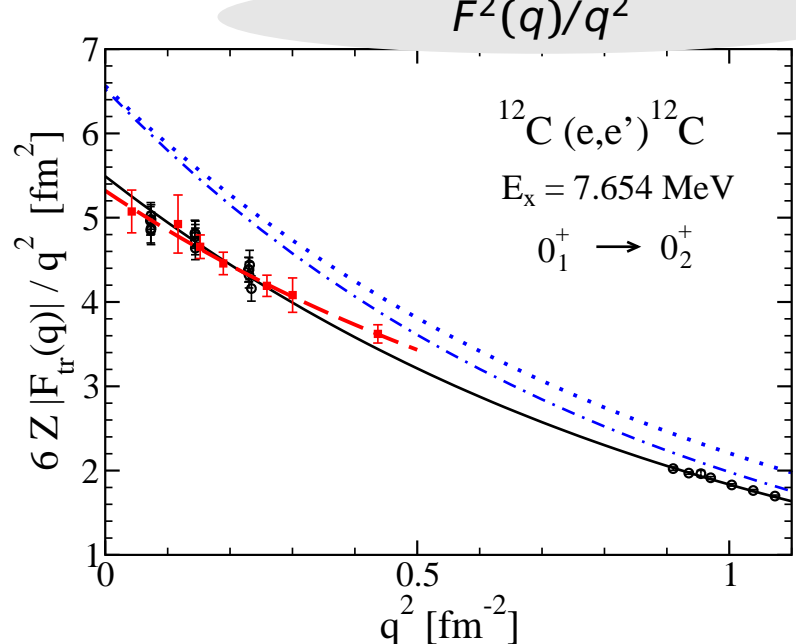
- ➔ elastic cross section described very well by FMD
- ➔ transition cross section better described by cluster model

$$\rho(\mathbf{x}) = \sum_{k=1}^A \langle \Psi | \delta(\tilde{\mathbf{x}}_k - \tilde{\mathbf{X}} - \mathbf{x}) | \Psi \rangle$$

- Cluster States in ^{12}C
- Monopole Matrix Element

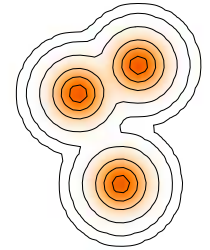
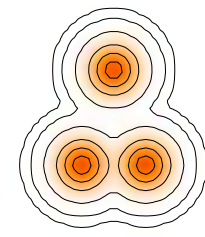
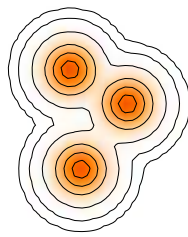
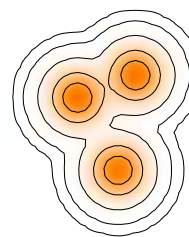


- $M(E0)$ determines the pair decay width
- model-independent self-consistent determination of transition form-factor/density in DWBA
- data at high momentum transfer necessary to constrain $M(E0)$ matrix element



- Cluster States in ^{12}C
- Important Configurations

- Calculate the overlap with FMD basis states to find the most important contributions to the Hoyle state



$$|\langle \cdot | 0_1^+ \rangle| = 0.94$$

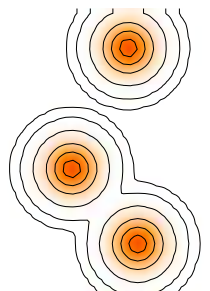
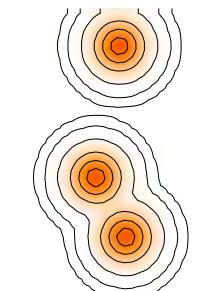
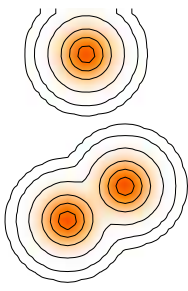
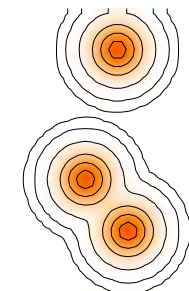
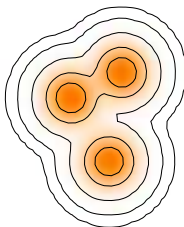
$$|\langle \cdot | 2_1^+ \rangle| = 0.93$$

$$|\langle \cdot | 0_2^+ \rangle| = 0.72$$

$$|\langle \cdot | 0_2^+ \rangle| = 0.71$$

$$|\langle \cdot | 0_2^+ \rangle| = 0.61$$

$$|\langle \cdot | 0_2^+ \rangle| = 0.61$$



$$|\langle \cdot | 3_1^- \rangle| = 0.83$$

$$|\langle \cdot | 0_3^+ \rangle| = 0.50$$

$$|\langle \cdot | 0_3^+ \rangle| = 0.49$$

$$|\langle \cdot | 0_3^+ \rangle| = 0.44$$

$$|\langle \cdot | 0_3^+ \rangle| = 0.41$$

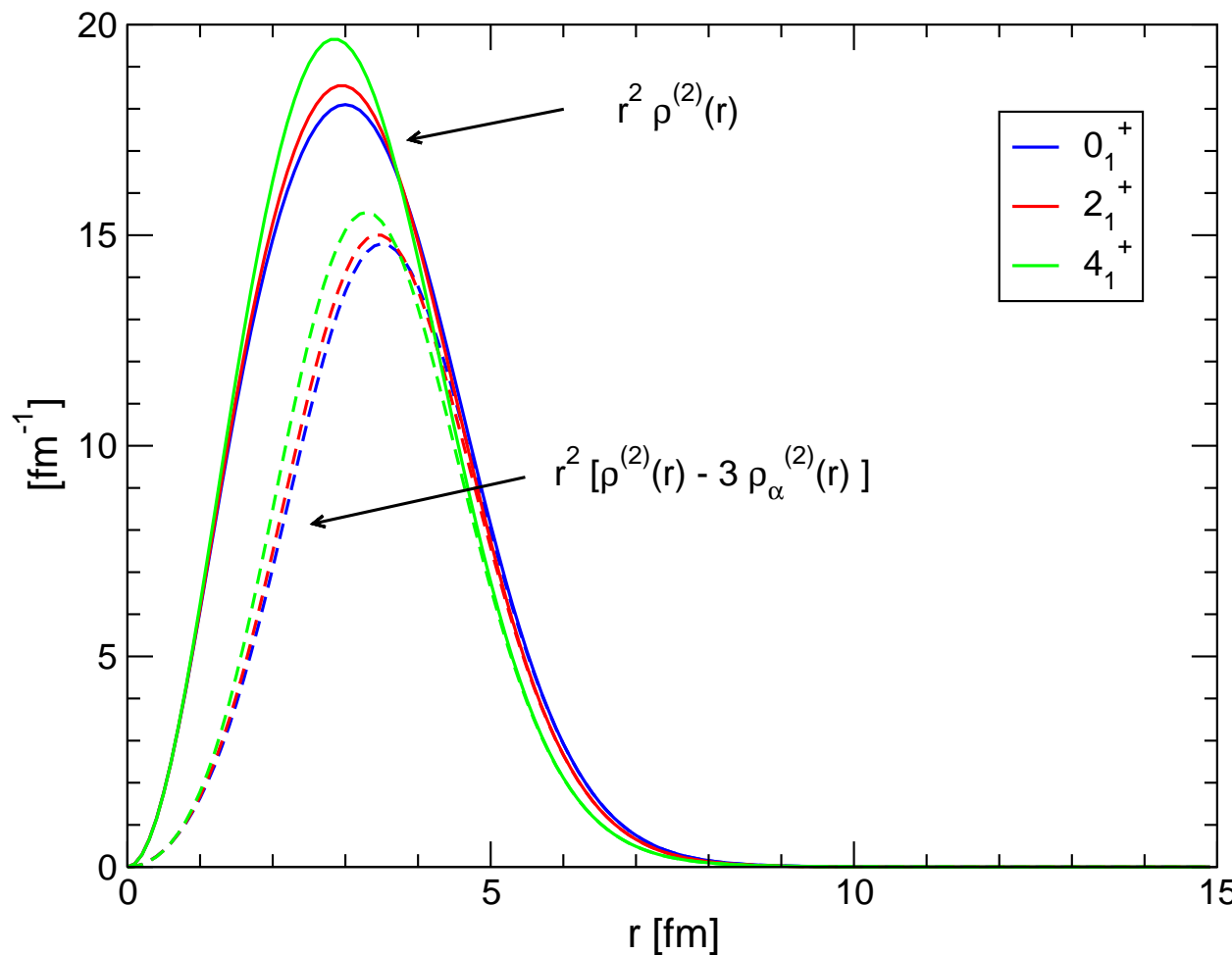
FMD basis states are not orthogonal!

0_2^+ and 0_3^+ states have no rigid intrinsic structure

- Cluster States in ^{12}C
- Two-body Densities and Intrinsic Structure

Cluster Model

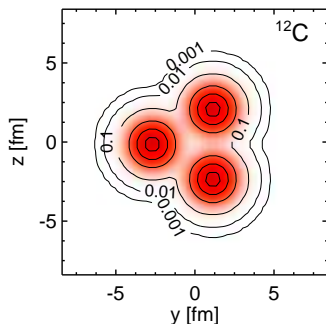
ground state band



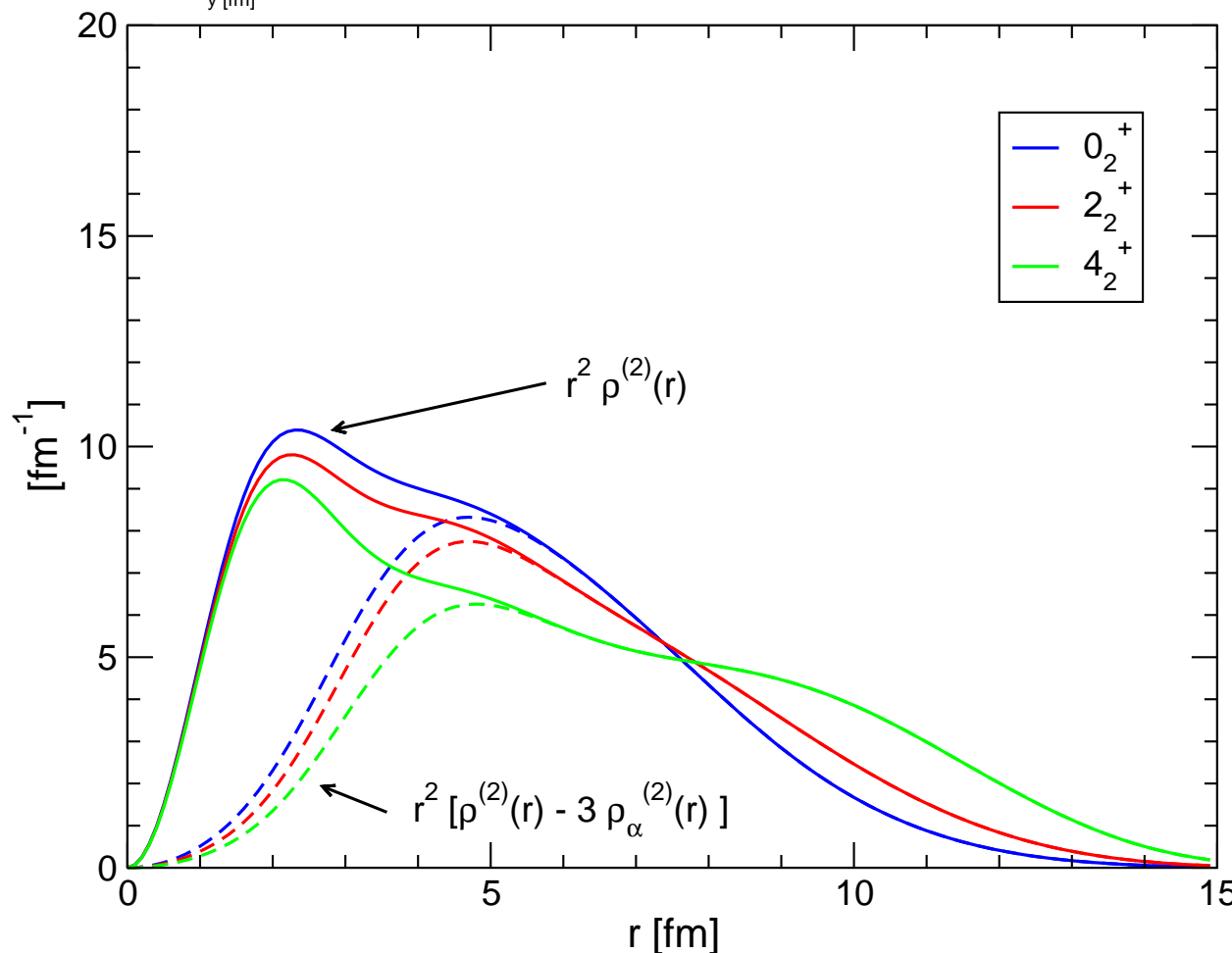
$$\rho^{(2)}(r) = \langle \Psi | \sum_{i < j} \delta(\mathbf{r} - \mathbf{r}_{ij}) | \Psi \rangle$$

- subtract contributions from α 's to extract “ α - α ” correlations
- (subtracted) two-body density peaks at 3.5 fm
- ➡ consistent with **compact triangular structure**

- Cluster States in ^{12}C
- Two-body Densities and Intrinsic Structure



Hoyle state "band"

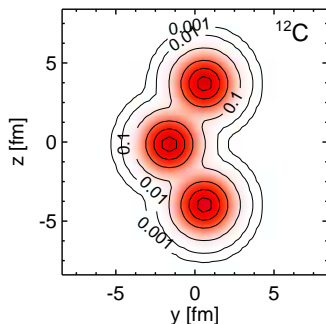


Cluster Model

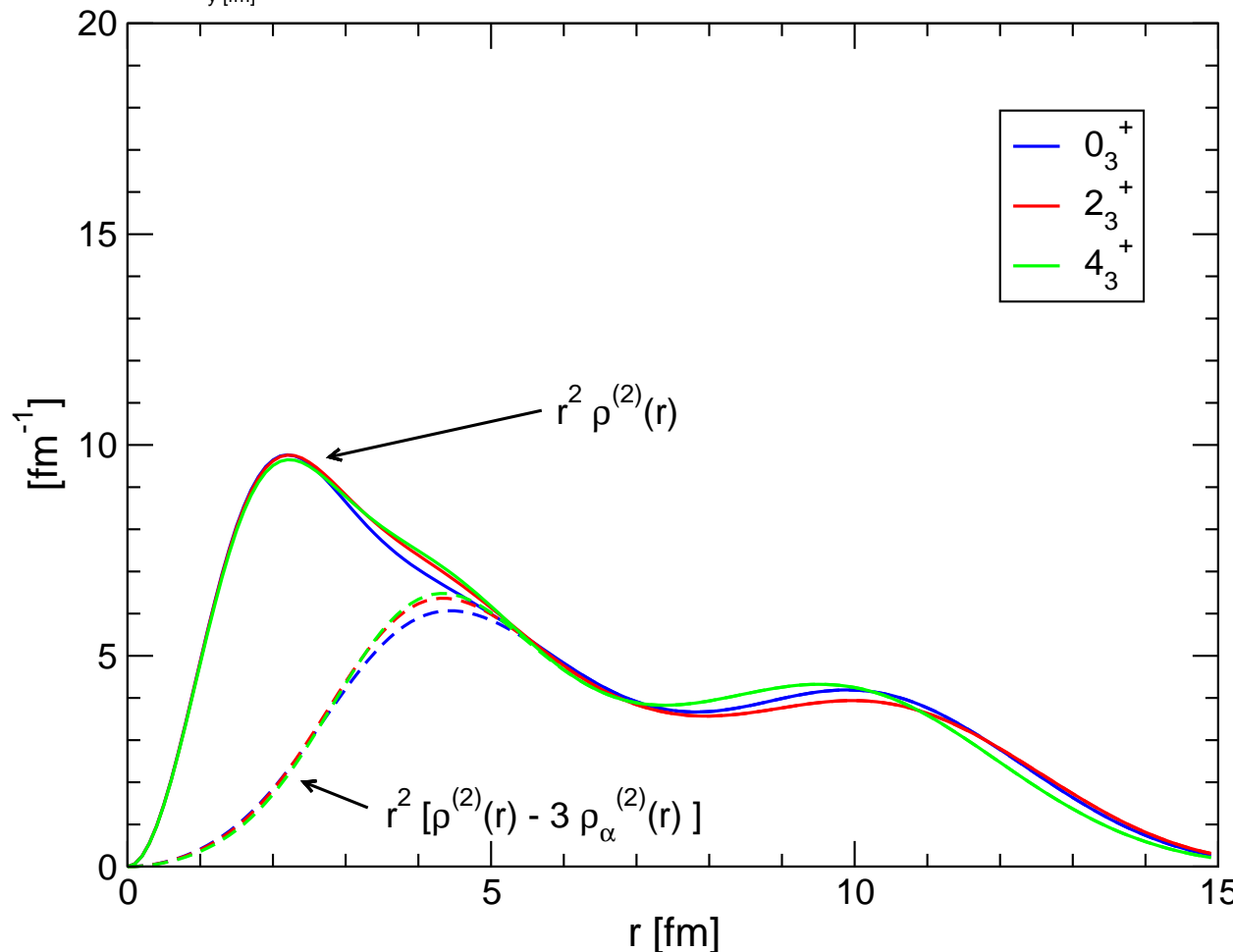
$$\rho^{(2)}(r) = \langle \Psi | \sum_{i < j} \delta(\mathbf{r} - \mathbf{r}_{ij}) | \Psi \rangle$$

- subtract contributions from α 's to extract “ α - α correlations”
- Hoyle state two-body density peaks at 5 fm, extended tail
- ➡ consistent with **triangular structure**
- tail in 2_2^+ and 4_2^+ states more pronounced
- ➡ admixture of open triangle configurations

- Cluster States in ^{12}C
- Two-body Densities and Intrinsic Structure



third 0^+ state band



Cluster Model

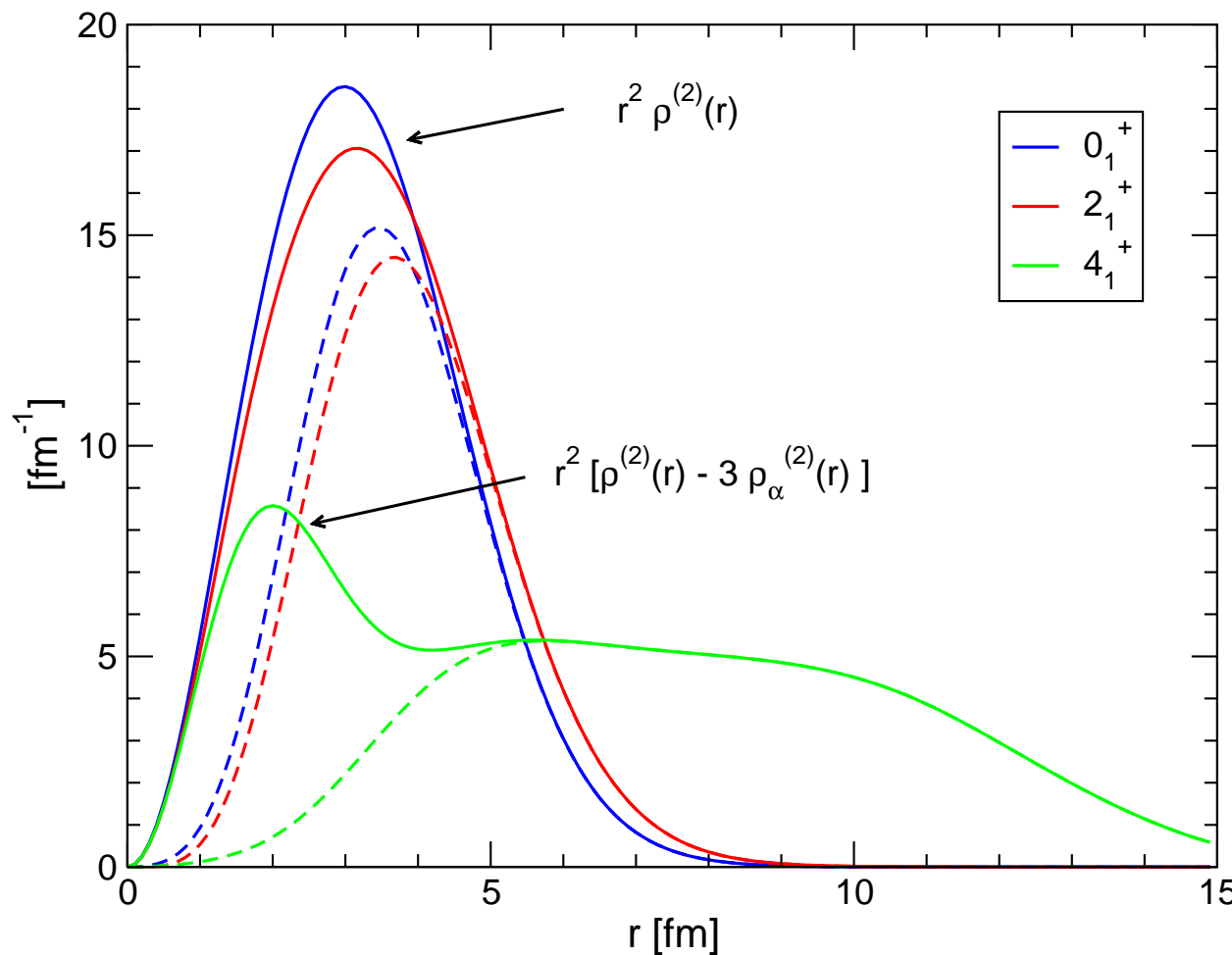
$$\rho^{(2)}(\mathbf{r}) = \langle \Psi | \sum_{i < j} \delta(\mathbf{r} - \mathbf{r}_{ij}) | \Psi \rangle$$

- subtract contributions from α 's to extract “ α - α ” correlations
- two-body density peaks at 4.5 fm and 10 fm
- ➡ consistent with **open triangle/chain configuration**

- Cluster States in ^{12}C
- Two-body Densities and Intrinsic Structure

FMD

ground state band



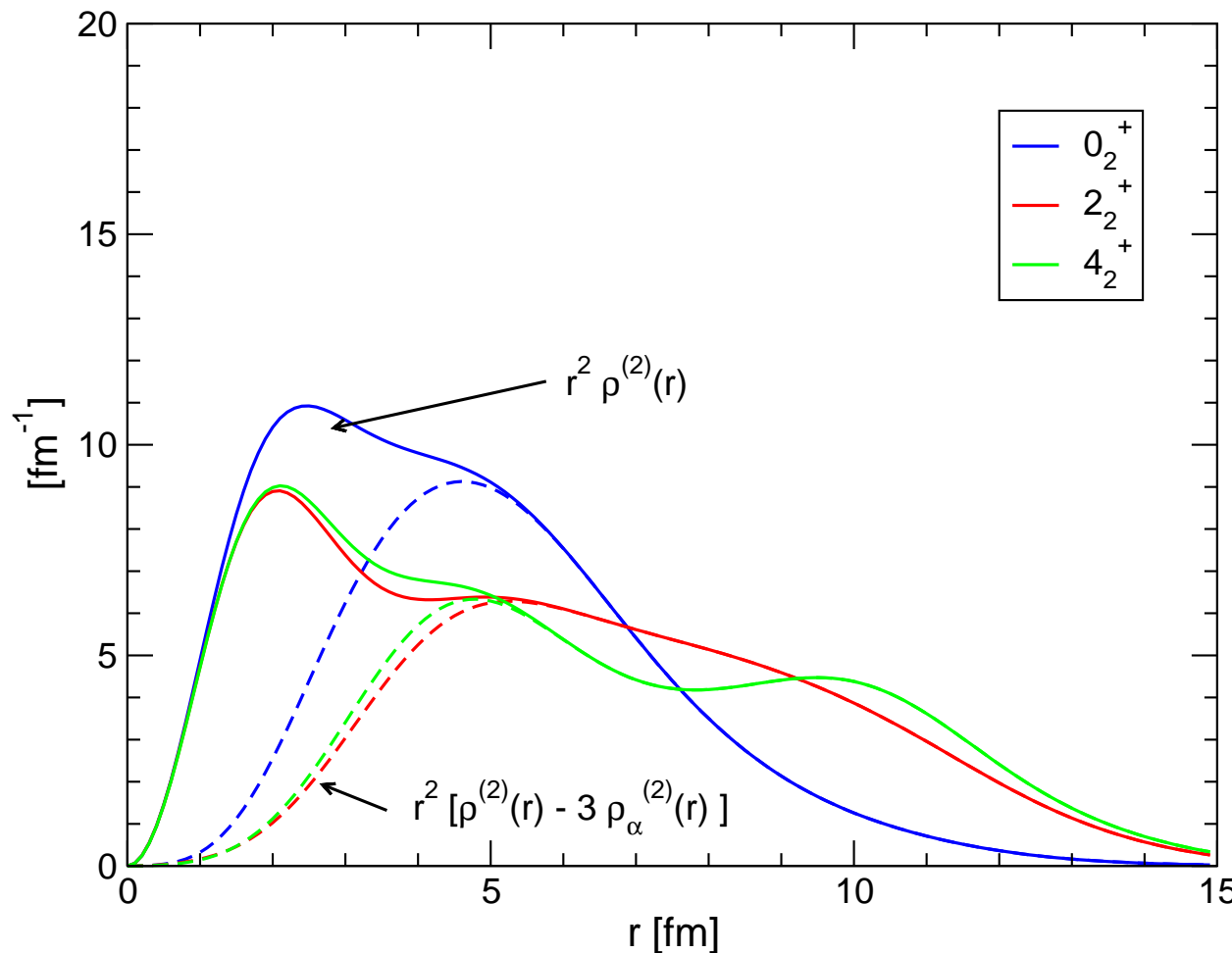
$$\rho^{(2)}(r) = \langle \Psi | \sum_{i < j} \delta(\mathbf{r} - \mathbf{r}_{ij}) | \Psi \rangle$$

- subtract contributions from α 's to extract $\alpha\text{-}\alpha$ correlations
- (corrected) two-body density peaks at 3.5 fm for 0^+ and 2^+
- 4^+ state strongly mixed with cluster configurations

- Cluster States in ^{12}C
- Two-body Densities and Intrinsic Structure

FMD

Hoyle state "band"

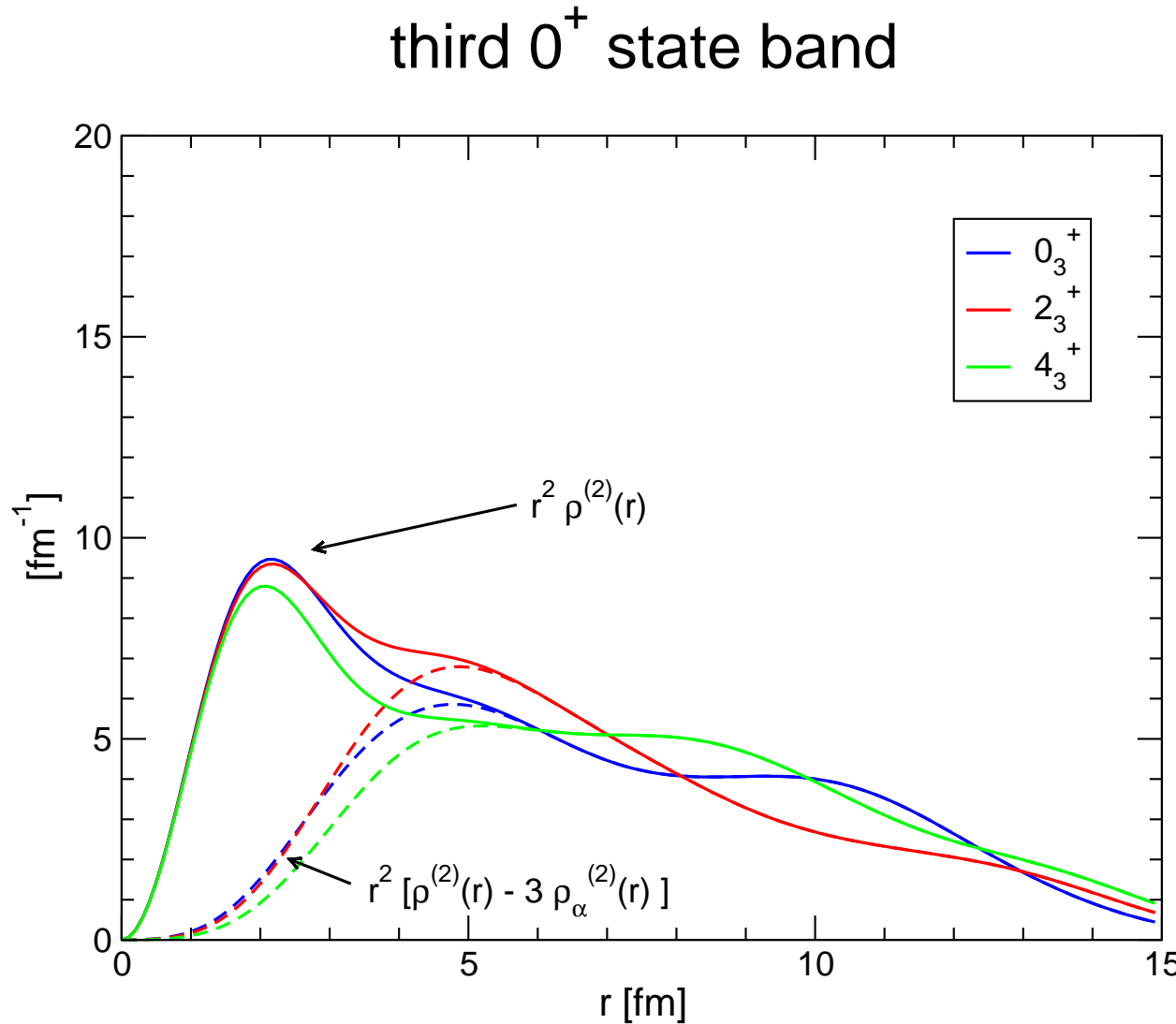


$$\rho^{(2)}(r) = \langle \Psi | \sum_{i < j} \delta(\mathbf{r} - \mathbf{r}_{ij}) | \Psi \rangle$$

- subtract contributions from α 's to extract $\alpha\text{-}\alpha$ correlations
- Hoyle state two-body density peaks at 5 fm, extended tail
- ➡ consistent with **extended triangular structure**
- 2_2^+ and 4_2^+ states have different intrinsic structure
- ➡ admixture of open triangle configurations

- Cluster States in ^{12}C
- Two-body Densities and Intrinsic Structure

FMD



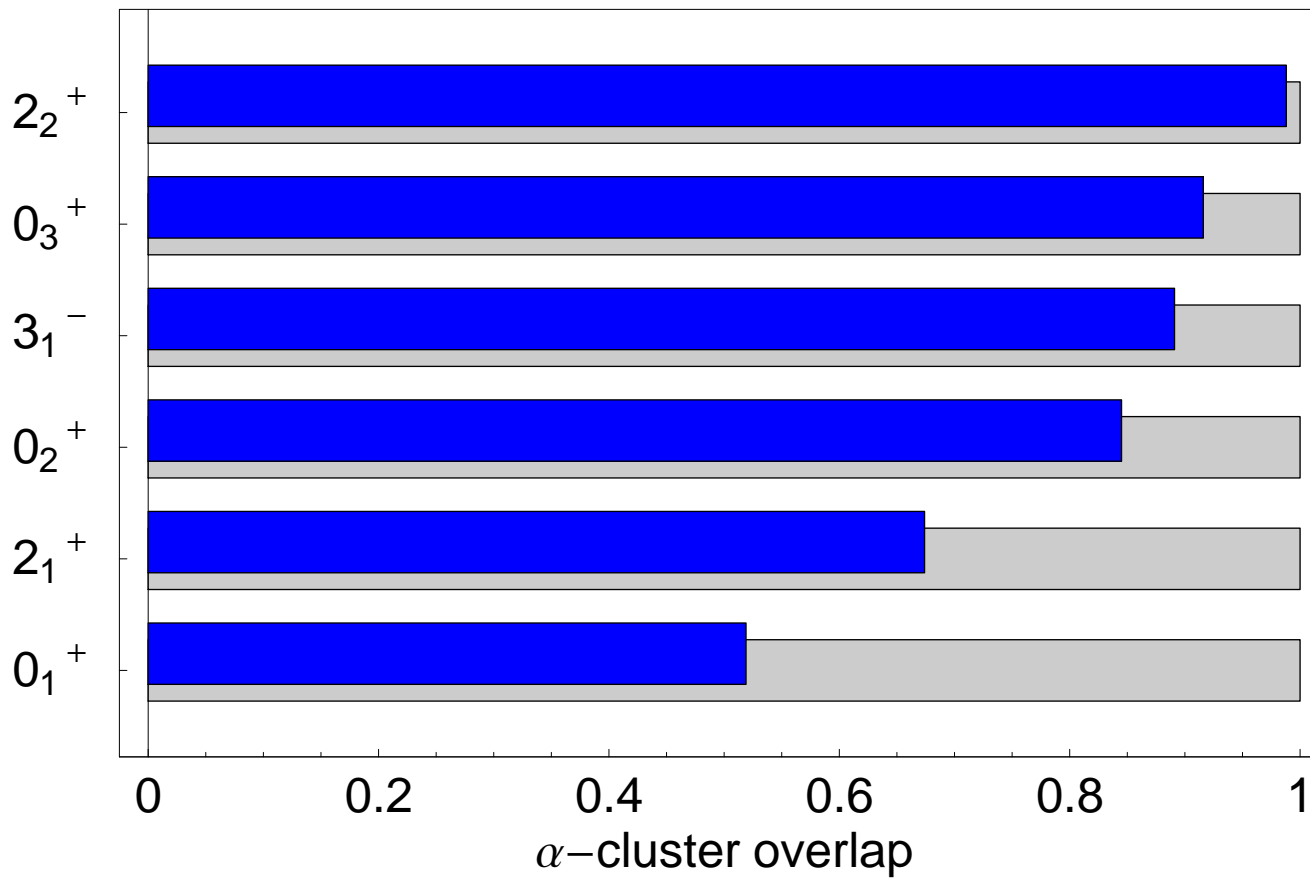
$$\rho^{(2)}(r) = \langle \Psi | \sum_{i < j} \delta(\mathbf{r} - \mathbf{r}_{ij}) | \Psi \rangle$$

- subtract contributions from α 's to extract $\alpha\text{-}\alpha$ correlations
- two-body density peaks at 4.5 fm and 10 fm
- ➡ consistent with **chain configuration**

- Cluster States in ^{12}C
- Overlap with Cluster Model Space

Calculate the overlap of FMD wave functions with pure α -cluster model space

$$N_\alpha = \langle \Psi | \tilde{P}_{3\alpha} | \Psi \rangle$$



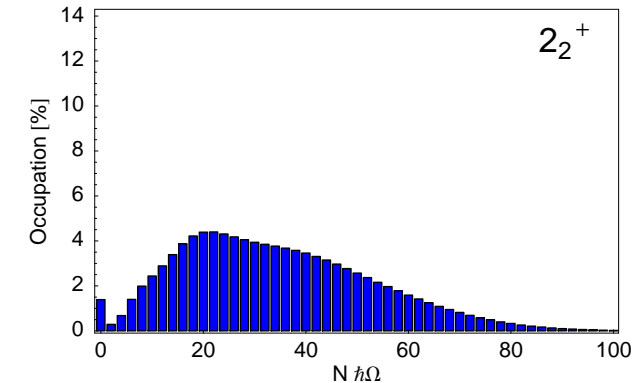
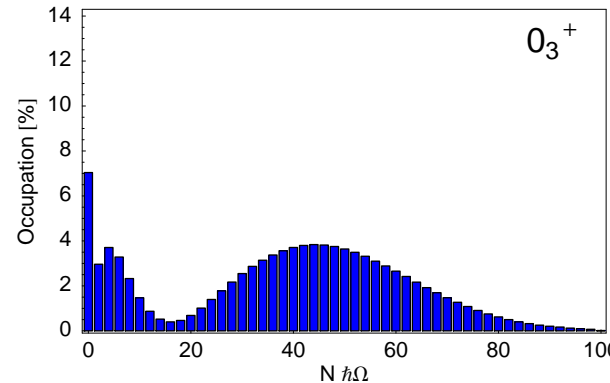
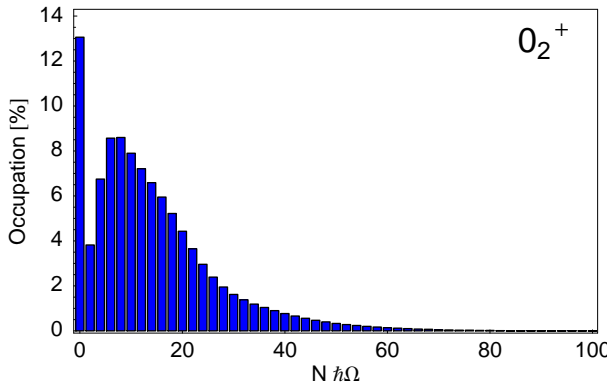
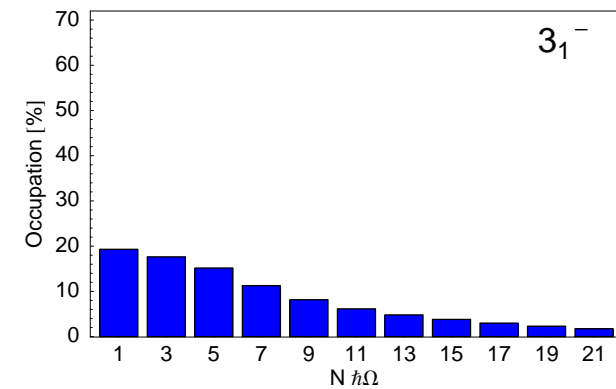
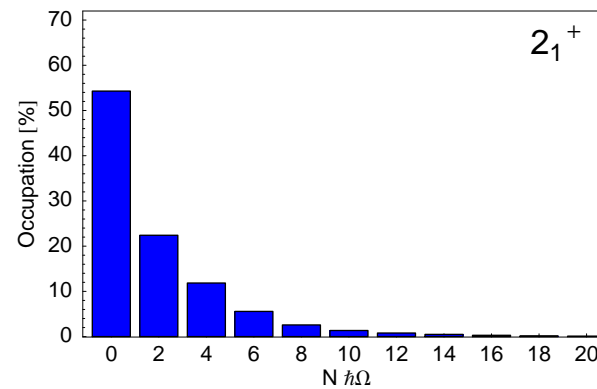
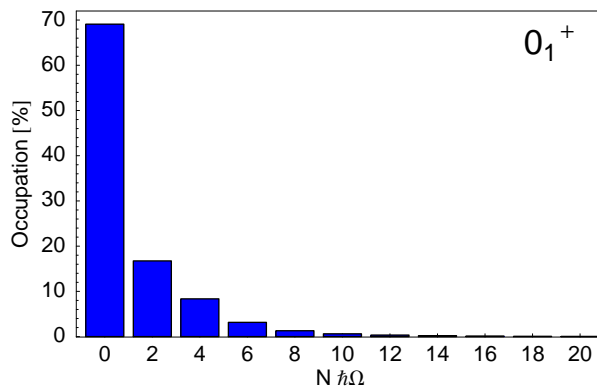
Hoyle state has 15% non-alpha admixtures

- Cluster States in ^{12}C
- Harmonic Oscillator $N\hbar\Omega$ Excitations

Y. Suzuki et al., Phys. Rev. C **54** 2073, (1996):

$$\text{Occ}(N) = \langle \Psi | \delta \left(\sum_i (\tilde{H}_i^{HO}/\hbar\Omega - 3/2) - N \right) | \Psi \rangle$$

FMD



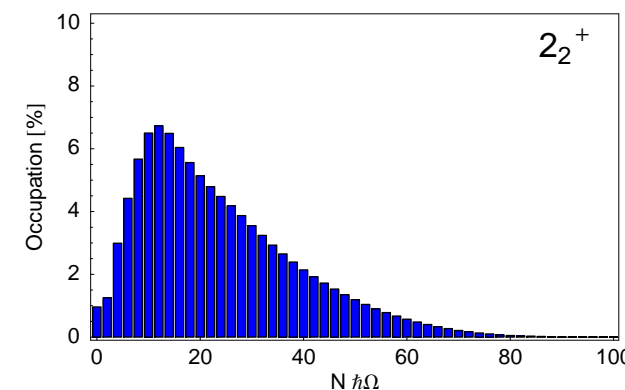
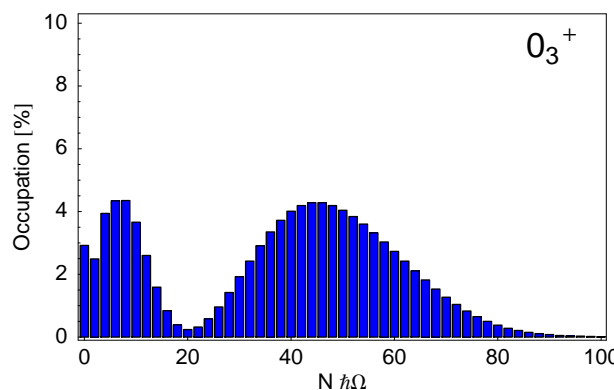
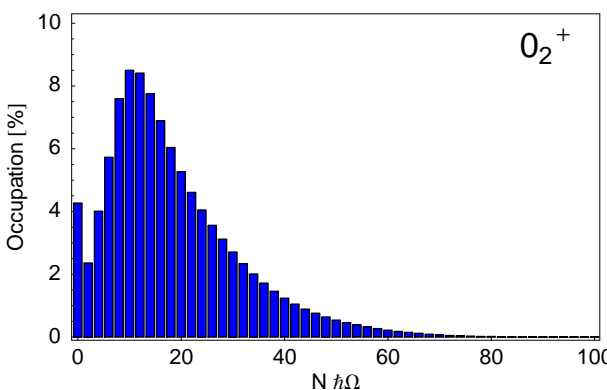
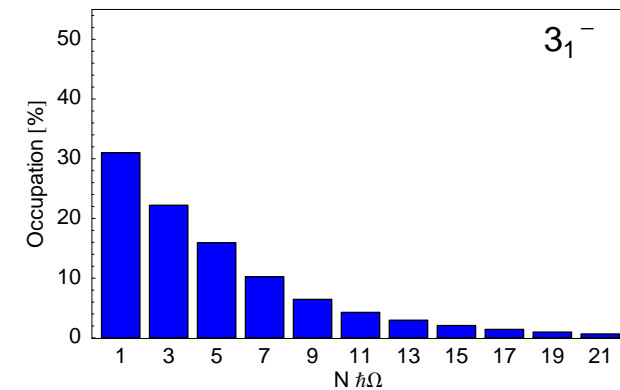
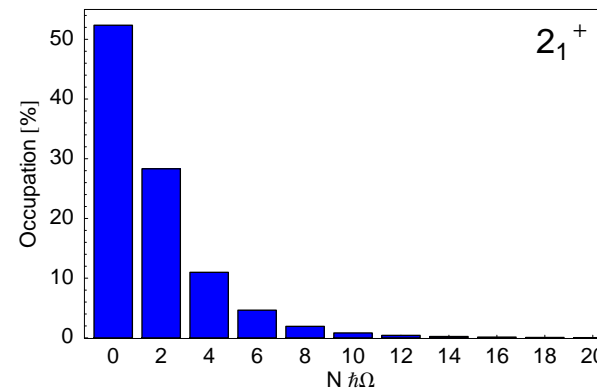
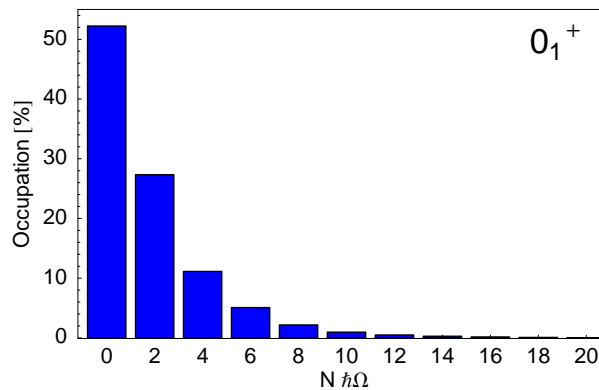
T. Neff, H. Feldmeier, Few-Body Syst. **45**, 145 (2009)

- Cluster States in ^{12}C
- Harmonic Oscillator $N\hbar\Omega$ Excitations

Y. Suzuki *et al*, Phys. Rev. C **54**, 2073 (1996).

$$\text{Occ}(N) = \langle \Psi | \delta \left(\sum_i (\tilde{H}_i^{HO}/\hbar\Omega - 3/2) - N \right) | \Psi \rangle$$

Cluster Model



Neon Isotopes ^{17}Ne - ^{22}Ne



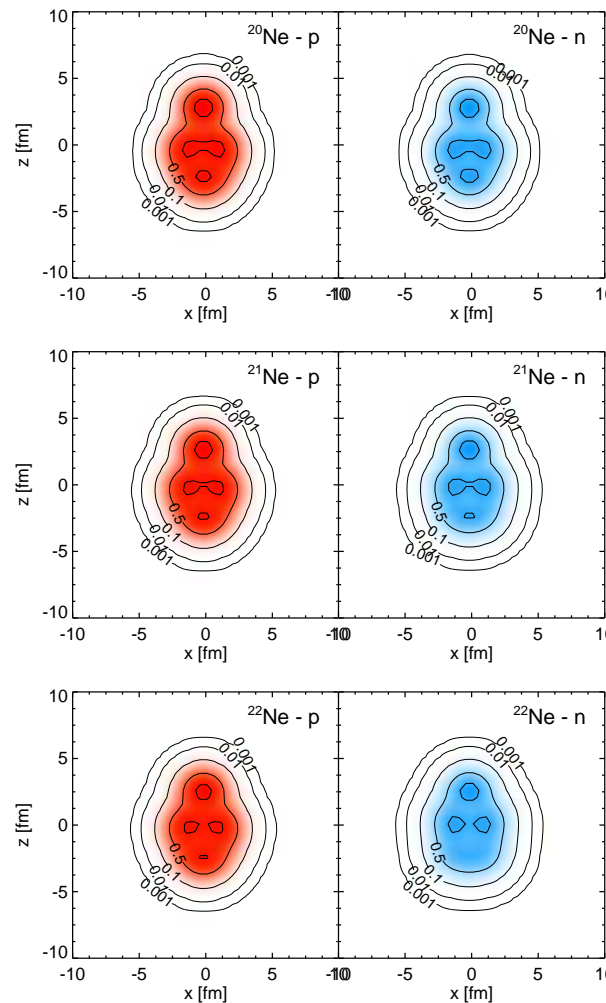
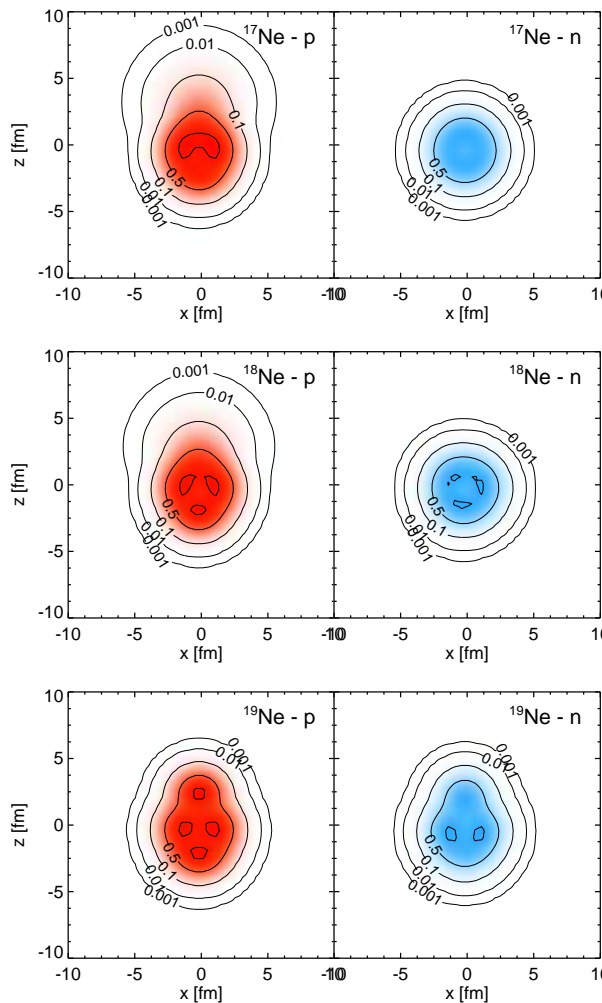
Structure ?

- s^2/d^2 competition in ^{17}Ne and ^{18}Ne
- ^3He and ^4He cluster admixtures

Observables

- » Charge Radii
- » Matter Radii
- » Electromagnetic transitions
- » Rotational bands

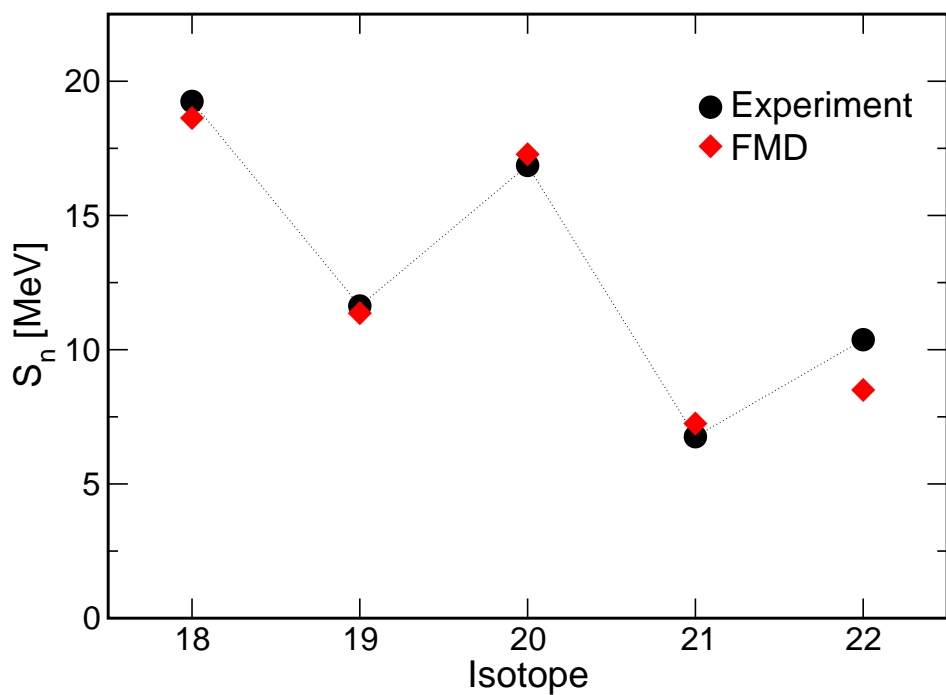
- Neon Isotopes
- Calculation



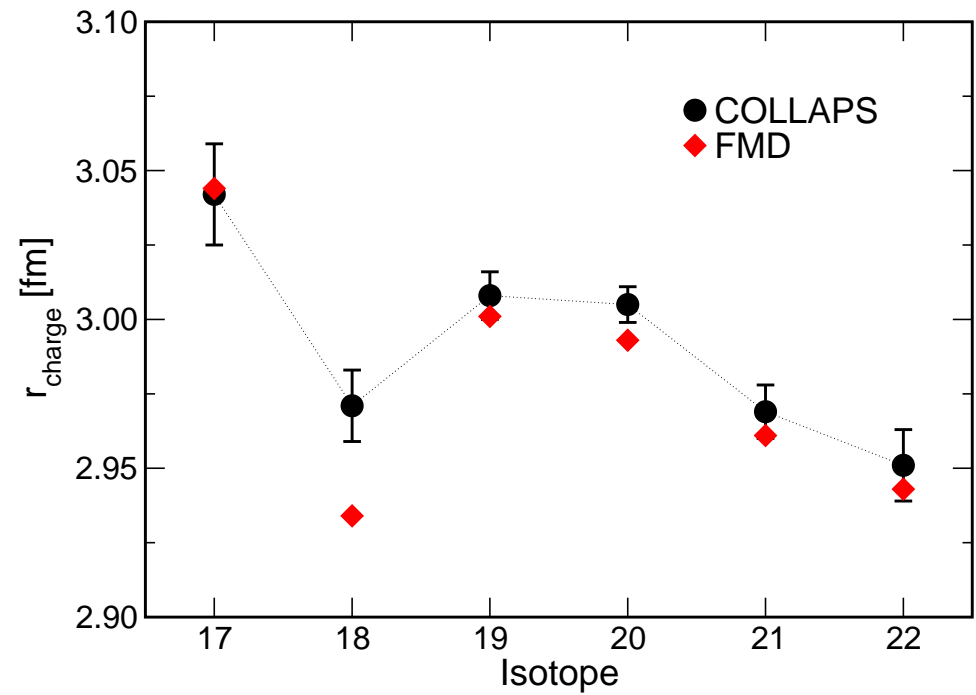
- two-body central and spin-orbit correction term added to realistic UCOM interaction – fitted to doubly magic nuclei
- Variation after parity projection on positive and negative parity
- Crank strength of spin-orbit force – changes properties of single-particle orbits and their occupations
- $^{15,16}\text{O}$ -“ s^2 ” and $^{15,16}\text{O}$ -“ d^2 ” minima in $^{17,18}\text{Ne}$
- explicit cluster configurations:
 ^{17}Ne : ^{14}O - ^3He
 ^{18}Ne : ^{14}O - ^4He
 ^{19}Ne : ^{16}O - ^3He and ^{15}O - ^4He
 ^{20}Ne : ^{16}O - ^4He
 ^{21}Ne : “ ^{17}O ”- ^4He
 ^{22}Ne : “ ^{18}O ”- ^4He

- Neon Isotopes
- Energies and Charge Radii

Separation Energies

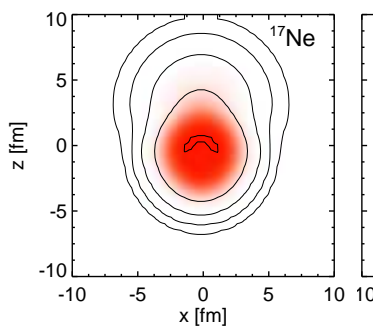


Charge Radii

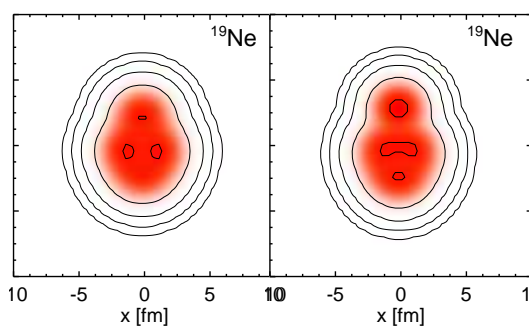


W. Geithner, T. Neff et al., Phys. Rev. Lett. **101**, 252502 (2008)

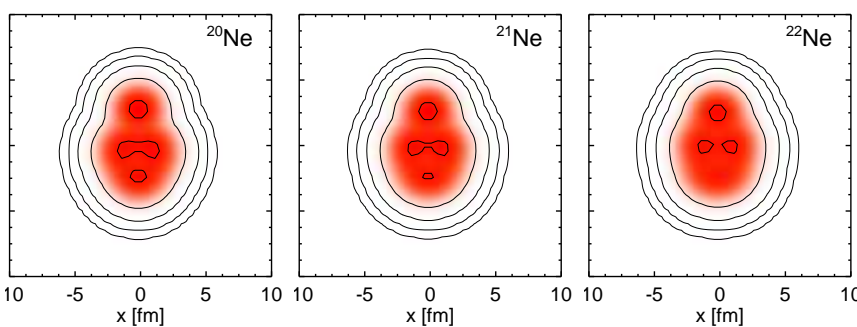
$^{17,18}\text{Ne}$: s^2/d^2 admixture



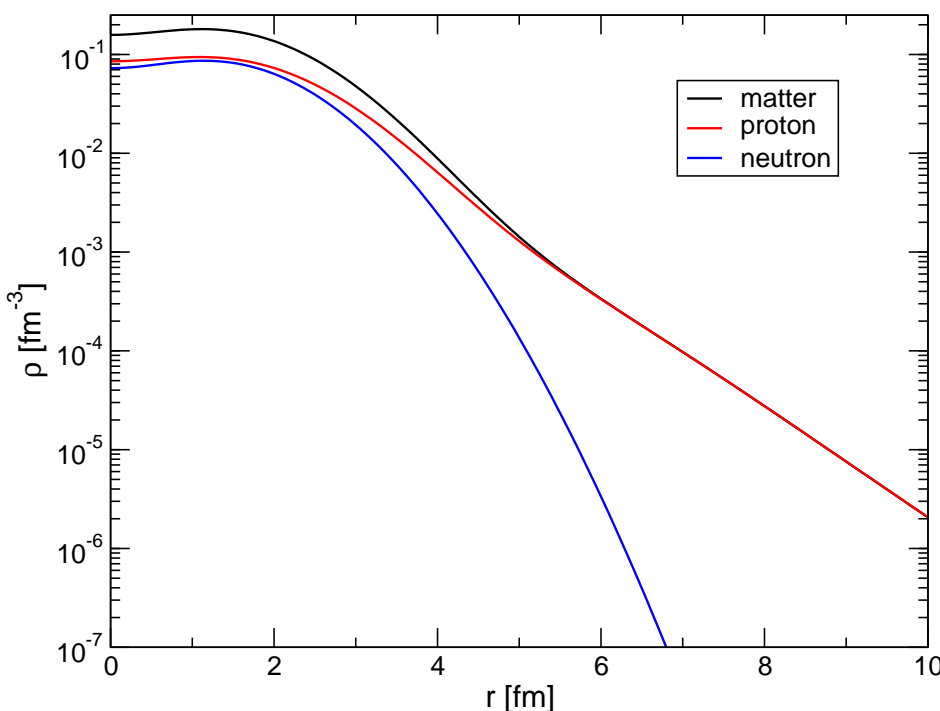
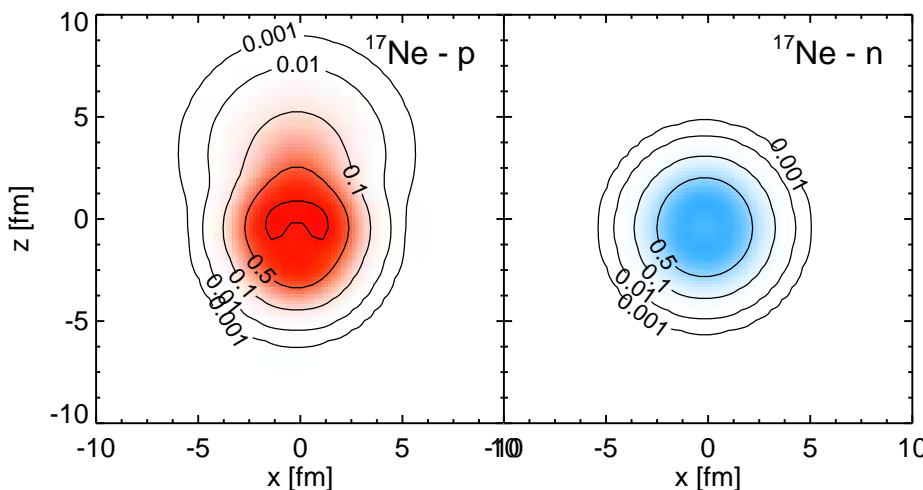
^{19}Ne : ^3He , α clustering



$^{20-22}\text{Ne}$: α clustering



- Neon Isotopes
- ^{17}Ne Halo ?



	FMD	Experiment
$r_{\text{ch}} [\text{fm}]$	3.04	$3.042(21)$
$r_{\text{mat}} [\text{fm}]$	2.75	$2.75(7)$ ¹
$B(E2; \frac{1}{2}^- \rightarrow \frac{3}{2}^-) [e^2 \text{fm}^4]$	76.7	66^{+18}_{-25} ²
$B(E2; \frac{1}{2}^- \rightarrow \frac{5}{2}^-) [e^2 \text{fm}^4]$	119.8	$124(18)$ ²
occupancy s^2	42%	
occupancy d^2	55%	

- proton skin $r_p - r_n = 0.45$ fm
- 40% probability to find a proton at $r > 5$ fm
- similar results are obtained in a three-body model

L. Grigorenko *et al.*, Phys. Rev. C **71**, 051604 (2005)

¹ A. Ozawa *et al.*, Nuc. Phys. **A693**, 32 (2001)

² M. J. Chromik *et al.*, Phys. Rev. C **66**, 024313 (2002)

Summary

Unitary Correlation Operator Method

- Explicit description of short-range central and tensor correlations
- Realistic low-momentum interaction V_{UCOM}

Fermionic Molecular Dynamics

Clustering and Localization – α - α wave function

$^3\text{He}(\alpha, \gamma)^7\text{Be}$ Radiative Capture

- Bound states, resonance and scattering wave functions
- S-Factor: energy dependence and normalization

Cluster States in ^{12}C

- Consistent description of ground state band and Hoyle state
- Two-body densities are a model independent tool for investigating structure
- Cluster states need tremendous model spaces in harmonic oscillator basis

Clustering in Neon isotopes

Thanks to my collaborators:

Hans Feldmeier (GSI), Wataru Horiuchi (Hokkaido), Karlheinz Langanke (GSI),
Robert Roth (TUD), Yasuyuki Suzuki (Niigata), Dennis Weber (GSI)